



*This page is left blank*

*This page is left blank*

---

**ABSTRACT**

The technique of Differential Scanning Calorimetry (DSC) has been applied to the characterization and the analysis of several activated carbons. These activated carbons included BPL carbon (a base carbon), ASC carbon (a BPL carbon impregnated with copper, chromium and silver) and ASC/T carbon (an ASC carbon impregnated with triethylenediamine, TEDA). DSC has been shown to be capable of measuring enthalpic changes associated with transitions and/or reactions of the surface species on the activated carbon. Physical changes or chemical reactions occurring on the carbon surface and the surface impregnants are observed as endotherms or exotherms (enthalpic changes) on the DSC curves (thermograms). The data from this study have demonstrated that DSC can be used quantitatively in the determination of the amount of TEDA impregnant on the activated carbon surface. This is based on the linear relationship between the area under the DSC curve and the amount of TEDA present. Qualitatively, DSC is shown to be able to differentiate between carbons which have been impregnated with different organic and/or metal impregnants, because each impregnated carbon produces a DSC thermogram which is unique to the compounds on its surface. This is due to the fact that different impregnants react with the carbon surface at different temperatures, thus giving rise to different DSC curves. It has also been found that activated carbons produced from different manufacturers showed different enthalpic characteristics.

## RÉSUMÉ

La technique de la calorimétrie à balayage différentielle (CBD) a été appliquée pour la caractérisation et l'analyse de plusieurs charbons de bois activés. Ces charbons activés incluaient le charbon BPL (un charbon de base), le charbon ASC (un charbon BPL imprégné avec du cuivre, du chrome et de l'argent) et le charbon ASC/T (un charbon ASC imprégné avec le triéthylenediamine, TEDA). La calorimétrie à balayage différentielle a démontrée être capable de mesurer les changements enthalpiques associés avec les transitions et/ou les réactions survenant à la surface du charbon activé. Les changements physiques ou les réactions chimiques qui surviennent à la surface du charbon et à la surface des imprégnants sont observés comme endotherme ou exotherme (changement enthalpiques) sur les courbes du DSC (thermogrammes). Les données de cette étude ont démontré que le DSC peut-être employé quantitativement dans la détermination de la quantité de l'imprégnant TEDA sur la surface du charbon activé. Ceci est basé sur la relation linéaire entre l'aire sous la courbe du DSC et le montant de TEDA présent. Qualitativement, le DSC a montré être capable de faire la différence entre les charbons qui ont été imprégnés avec des substances organiques différentes et/ou des imprégnants métalliques, parce que chacun des charbons imprégnés donne un thermogramme qui est unique aux composés chimiques à sa surface. Ceci est du au fait que chaque imprégnant réagit avec la surface du charbon à différentes températures, et par conséquent donnant lieu à différentes courbes DSC. Il a été aussi trouvé que le charbon activé produit par différents fabricants ont montrées des caractéristiques enthalpiques différentes.

### EXECUTIVE SUMMARY

Activated carbon and its impregnated varieties (such as ASC carbon, which contains copper, chromium and silver as the active impregnants, or ASC/T, an ASC carbon which also contains TEDA, triethylenediamine) have been employed in military respiratory protection against air-borne contaminants and toxic materials. To date, only a few spectroscopic techniques have been applied to the study and the characterization of these activated carbons.

A thermal analytical technique, Differential Scanning Calorimetry (DSC), is employed in this study to characterize several activated carbons. Physical changes and chemical reactions between the impregnants and the carbon surface occur when the carbon is being heated progressively to higher temperatures. DSC is designed to monitor these reactions and changes, which give rise to heat flows (enthalpic changes), varying with the temperature.

In this study, the DSC has been shown to be useful in the quantitative determination of the amount of TEDA on ASC/T carbon, since the area under the DSC curve bears a linear relationship to the amount of TEDA present. The results from this study also indicated that DSC can be used qualitatively to distinguish impregnated carbons from each other, e.g. impregnated carbons from different manufacturers, or carbons which are impregnated differently. Since each surface species responds differently to DSC, every thermogram (or DSC curve) is distinct, and is characteristic of the impregnated carbon.

**TABLE OF CONTENTS**

	<u>Page</u>
<b><u>ABSTRACT/RÉSUMÉ</u></b> . . . . .	iii
<b><u>EXECUTIVE</u></b> . . . . .	v
<b>1.0 <u>INTRODUCTION</u></b> . . . . .	1
<b>2.0 <u>THE THEORY AND OPERATION OF DIFFERENTIAL SCANNING CALORIMETRY</u></b> . . . . .	2
<b>2.1 THERMOANALYTICAL TECHNIQUES</b> . . . . .	2
<b>2.2 OPERATIONS OF DSC</b> . . . . .	4
<b>3.0 <u>EXPERIMENTAL</u></b> . . . . .	6
<b>3.1 THE OPERATION OF THE DIFFERENTIAL     SCANNING CALORIMETER</b> . . . . .	6
<b>3.1.1 <u>Estimation of Experimental Errors</u></b> . . . . .	6
<b>3.1.2 <u>Peak Area Measurement</u></b> . . . . .	6
<b>3.2 MOISTURE CONTENT DETERMINATION OF CARBON</b> . . . . .	7
<b>3.3 PREPARATION OF SAMPLES FOR INORGANIC     IMPREGNANT ANALYSIS</b> . . . . .	7
<b>3.4 PREPARATION OF SAMPLES FOR ORGANIC     IMPREGNANT ANALYSIS</b> . . . . .	7
<b>4.0 <u>RESULTS AND DISCUSSION</u></b> . . . . .	8
<b>4.1 ERRORS ASSOCIATED WITH THE DSC INSTRUMENT</b> . . . . .	8
<b>4.1.1 <u>Temperature Measurements</u></b> . . . . .	8
<b>4.1.2 <u>Area Under the DSC Curve</u></b> . . . . .	10
<b>4.1.3 <u>Consistency of the DSC Curves</u></b> . . . . .	10
<b>4.2 TYPICAL DSC CURVES FOR CALGON CARBONS</b> . . . . .	12
<b>4.3 INORGANIC IMPREGNANTS ON ASC CARBON</b> . . . . .	13
<b>4.4 ORGANIC IMPREGNANTS (TEDA) ON CARBON</b> . . . . .	15
<b>4.4.1 <u>DSC Thermograms of BPL and ASC Carbons         Impregnated with TEDA</u></b> . . . . .	15
<b>4.4.2 <u>Quantitative Analysis of TEDA Content         on Carbon by DSC Measurements</u></b> . . . . .	16

**TABLE OF CONTENTS** (Cont'd)

	<b><u>Page</u></b>
4.5 OTHER ORGANIC IMPREGNANTS . . . . .	18
4.6 IMPREGNATED CARBONS FROM OTHER SOURCES . . . . .	20
5.0 <b><u>CONCLUSIONS</u></b> . . . . .	20
6.0 <b><u>REFERENCES</u></b> . . . . .	22
<b><u>ANNEX A: MOISTURE CONTENT DETERMINATION OF CARBON BY DSC</u></b> . .	A-1

## 1.0 INTRODUCTION

Activated carbon is employed as a universal adsorbent for the removal of a variety of organic and inorganic materials in contaminated air and water. The large adsorption capacity on the carbon surface and the associated porous microstructure facilitate the adsorption process whereby all the undesirable materials are retained. For military deployment, the activated carbon is impregnated with metallic salts of copper, chromium and silver, the so-called ASC whetlerite (1), and sometimes also with organic compounds such as triethylenediamine (TEDA), known as the ASC/T carbon (2). These added impregnants improve the chemical reactivity of the activated carbon in the removal of some toxic gases such as hydrogen cyanide (AC), cyanogen chloride (CK), and phosgene (CG). It is believed that these impregnants either react with or catalytically convert all these toxic substances into innocuous products. TEDA is also known to prolong the service life of the impregnated carbon by reducing the amount of adsorbed water, thus lessening the effect of ageing. The ASC/T carbon is the current adsorbent of choice employed in the Canadian gas-mask canisters.

In the course of the research and development on activated carbon carried out in this laboratory, it is essential to be able to characterize the impregnated carbon, and to correlate its properties with the observed activities. This is especially important in the search for new impregnation formulations for the carbon. For base carbon (i.e. activated carbon without any impregnants), the physical characterization consists of the determination of the surface area, pore volume and pore size distributions, and adsorption capacity (water and organics, such as carbon tetrachloride) etc. However, for the impregnated carbon, the techniques mentioned above could not reveal the complete chemical profile (i.e. structure, distribution and reactivities) of the impregnants and the impregnated carbon surface. Similarly, wet chemistry analytical techniques reveal very little information except the concentration of the impregnants existing on the carbon surface.

The application of modern spectroscopic techniques to the study of activated carbon (base and impregnated) has met with limited success, due to the inherent properties of the activated carbon. For example, due to the opaqueness of the carbon, infra-red, ultra-violet and other spectroscopies which require light transmission through the sample are useless. Fourier-transform infra-red (FTIR) equipped with expensive accessories such as photo-acoustic detection or diffuse-reflectance lens systems are necessary to extract very limited information from the surface structure on the carbon (3). Solid-state  $^1\text{H}$  and  $^{13}\text{C}$  nuclear magnetic resonance with magic angle spinning has also been attempted in this laboratory in the study of carbon surface with very little success (3). This is due, first to the large dipolar



coupling (between the carbons and between the carbon and hydrogen), and secondly to the paramagnetic species (such as  $\text{Cu}^{++}$ ) present on the impregnated carbon surface which further broadens the resonances. A study of magnetic properties has been carried out in this laboratory (4) and by others (5), which revealed nothing more than the oxidation states of the impregnants. So far, only surface analytical techniques have been shown to be successful in the study of carbon surface. Auger, X-ray photoelectron spectroscopy (XPS) and transmission electron microscopies (6-8) have been shown to provide a wealth of information about the surface structure and the distribution of surface species, as deep as about 20Å from the carbon surface. However, these surface analytical services are expensive, and the interpretation of the resulting spectra requires expertise in this field.

The technique of Differential Scanning Calorimetry (DSC) has recently been employed at DREO in the determination of moisture content on several activated carbons with reasonable success (9). The activated carbons studied include a BPL carbon (a base carbon, 12 x 30 US mesh size), an ASC (a BPL carbon which has been impregnated with copper, chromium and silver) and an ASC/T (an ASC carbon further impregnated with triethylenediamine, TEDA). During the progress of this moisture determination study, it has become apparent that the technique of DSC has not been utilized to its fullest potential, as documented in the literature (10). This report details the further effort in exploring the feasibility of using DSC as an analytical tool for determination of:

- (1) the identity and concentrations of the metal impregnants,
- (2) the identity and concentrations of the organic impregnants,
- (3) the original precursor (coal-based or coconut-shell), manufacturer, and the impregnation history.

## 2.0 THE THEORY AND OPERATION OF DIFFERENTIAL SCANNING CALORIMETRY (11-13)

### 2.1 THERMOANALYTICAL TECHNIQUES

This section of the report will describe very briefly an analytical technique which continuously monitors physical and/or chemical changes of a sample which occur as the temperature is varied. This thermoanalytical technique consists of three principal methods: Thermogravimetry (TG), Differential Thermal Analysis (DTA) and Differential Scanning Calorimetry, and only the latter one will be discussed here. The theoretical basis of thermal analysis may be approached from either a kinetic or thermodynamic viewpoint. Kinetically, the Arrhenius equation will apply:

$$\text{Rate} = A \exp (- \Delta E/RT ) \quad [1]$$

where A,  $\Delta E$ , R and T stand for the pre-exponential factor, activation energy, gas law constant and temperature respectively. This equation indicates that reaction rates increase with temperature. At some point the rate becomes significant (i.e. it has overcome the activation energy barrier), and a chemical or physical change occurs. Similarly, the Gibbs free energy equation:

$$\Delta G^\circ = \Delta H^\circ - T\Delta S^\circ \quad [2]$$

where  $\Delta G^\circ$  is the Gibbs free energy,  $\Delta H^\circ$  is the reaction enthalpy, and  $\Delta S^\circ$  and T are the entropy change for the process and the temperature respectively, shows that the equilibrium constant, K which relates to  $\Delta G^\circ$  as follow:

$$\Delta G^\circ = - RT \ln K \quad [3]$$

will change with temperature. If  $\Delta S$  is positive and temperature has increased, the equilibrium will be shifted to favour the formation of products. In many cases, a combination of these causes the observed physicochemical process.

Instrumentation for thermoanalysis requires appropriate sample and reference holders enclosed in an oven equipped with a temperature-programming device and the necessary transducer for converting the physicochemical property being measured into electrical signals. A schematic of the Dupont DSC employed in this study is reproduced in Figure 1, and will be discussed in detail in Section 2.2. Samples may be studied in air or other atmospheres, inert or reactive, at reduced, ambient or elevated pressures. Exact experimental conditions are chosen to enhance the process under study and ensure reproducibility. Selection of experimental parameters includes heating rate, temperature range, atmospheric composition and pressure, recorder attenuation and speed, and sample preparation. Each of these may affect the thermograms produced.

Thermograms are plots of measured heat evolved versus the oven temperature. Under rigorously controlled conditions, DSC curves uniquely represent the system under study. Melting, crystallization, decomposition, oxidation, reduction, adsorption, absorption, desorption, polymerization reactions and heat capacity changes are observable on the DSC curves.

## 2.2 OPERATIONS OF DSC (14,15)

Differential Scanning Calorimetry (DSC) is a thermo-analytical method which is based on the enthalpic change in a material. Two types of DSC instruments have been widely used: the Heat Flux DSC (e.g. the Du Pont 910 DSC described in this report), and the Power Compensated DSC.

The schematic of a Du Pont 910 DSC cell is shown in Figure 1. The cell uses a constantan disk as its primary means of heat transfer to the sample and reference positions and as one element of the temperature measuring thermoelectric junctions. The sample of interest and a reference are placed in aluminum pans that sit on raised platforms on the constantan disk. Heat is transferred from the disk and up to the sample and the reference via the sample pans. The differential heat flow to the sample and the reference is monitored by chromel-constantan thermocouples formed by the constantan disk and a chromel wafer that covers the underside of each platform. Chromel and alumel wires are connected to the underside of the constantan wafers, and the resultant chromel-alumel thermocouple is used to monitor the sample temperature directly. Constant calorimetric sensitivity is maintained throughout the usable range of the cell via electronic linearization of the cell calibration coefficient E. Temperature ranges from  $-180^{\circ}\text{C}$  to  $725^{\circ}\text{C}$  are possible in inert atmospheres ( $600^{\circ}\text{C}$  maximum in oxidizing atmospheres). Since the Power-Compensated DSC cell was not employed, its operation will not be discussed here. Interested readers should refer to References 11-13 and 15 for greater detail.

In the simplest terms, the analytical method involving a DSC cell can be expressed as follows. A sample and a reference are individually heated, by separately controlled resistance heaters, at a pre-determined rate while they are kept isothermal. Enthalpic processes are detected as differences in electrical energy needed to produce this desired isothermal heating rate. This electrical energy, in milli-calories per second, is then plotted versus the sample temperature to obtain the thermogram (this is denoted as a DSC curve in the text). The most important point to note is: the DSC process measures the difference in energy inputs into a substance and a reference (a blank in our case). This difference is measured as a function of temperature, while the substance and reference material are subject to a controlled temperature program.

A typical DSC curve is depicted in Figure 2. The baseline of the thermal curve is defined when the differential net flow, segments AB and DE, is approximately zero. The peak is defined as the part of the curve that rises from the baseline and returns to it (e.g. segments BCD and EFG). An exothermal peak is defined when the differential heat flow is positive, as in segment BCD. The sample's temperature tends to rise above the temperature of the reference material as it gives off heat compared to the reference

sample. An endothermal peak is defined when the differential heat flow is negative, as in segment EFG. The sample's temperature tends to fall as it adsorbs heat compared to the reference sample. All heat transfer between the sample and reference materials occurs as a result of chemical or physical change of the sample. A glass transition is defined as the temperature at which an amorphous solid becomes rubbery. This physical change is observed as a change in the baseline (point A) and is due to a change in the heat capacity of the sample. The total enthalpy change associated with the peak is calculated based upon the area under the peak. The melting point is represented by the segment EFG on the DSC curve. It occurs in an endothermic transition. The temperature onset (point E) is considered the melting point of the sample. For more complicated curves, the DSC's analytical programs determine where one peak ends and the onset of the next peak occurs. An example of this may be observed in Figure 3, where the end of the endothermic peak and the point at which the first exothermic peak begins was determined.

To determine the transition peak area for a specific section of a DSC curve, a built-in data analysis program integrates over the desired area (14). The computer software determines the onset point of a peak by noting the change in the slope of the baseline (denoted on Figure 3 as A). Point B, the end-point of the peak, is determined similarly. The tangents from the baseline originating from points A and B are drawn, and intercept at C. Extrapolating back from C towards the baseline yields the point D. The computer then draws a line connecting the points A and D. These two points are entered manually by the operator. The computer program then calculates the total peak area (indicated by hatching) enclosed by this artificial line and the enthalpic change with the following equation:

$$\Delta H = A (60BE\Delta q_s) / m \quad [4]$$

where:

$\Delta H$  = heat of reaction in Joules/g  
 $A$  = peak area in  $\text{cm}^2$   
 $m$  = sample mass in mg  
 $B$  = time base Scaling in min/cm  
 $E$  = cell calibration coefficient at the temperature of the experiment (dimensionless)  
 $\Delta q_s$  = Y-axis scaling in mW/cm

The quantity  $(60BE\Delta q_s)$  is an instrumental constant which is characteristic of the experimental condition. It is generally used to convert the measured area directly into heat of reaction.  $E$  is a calibration constant which can be determined from running an indium standard.

### 3.0 EXPERIMENTAL

The activated carbons employed in this study were obtained from three sources: Calgon Carbon Corporation, Pittsburgh, USA, Norit N.V. Netherlands, and Sutcliffe-Speakman, UK. From the Calgon source, three different types of carbons were studied: BPL (Lot number 937-YB), ASC (Lot Numbers 1048, 1715, and 1746), and ASC/TEDA (Lot number 947). Only ASC and ASC type carbons were studied for the Norit and Sutcliffe-Speakman sources respectively. Samples of all these carbons were analyzed as received. All chemicals used were purchased from Aldrich Chemical Co., Milwaukee, USA.

#### 3.1 THE OPERATION OF THE DIFFERENTIAL SCANNING CALORIMETER

A Du Pont 2100 Thermal Analyst was used to control the 910 Differential Scanning Calorimeter. Approximately ten to twenty milligrams of carbon granules were placed inside a 40- $\mu$ L aluminum pan which was then encapsulated with an aluminum cap. The reference pan was a similar, but empty aluminum pan. All experiments were performed under a flow of dry nitrogen at 100 mL/min. A temperature enthalpy analysis was carried out between 25°C and 600°C at a heating rate of 30°C/min. The data was stored on a floppy disk and processed with a microcomputer.

THE 910 DSC cell and the temperature were calibrated every two weeks or whenever the baseline started to shift, according to standard procedure (14).

##### 3.1.1 Estimation of Experimental Errors

This experiment was designed to estimate the experimental reproducibility of DSC measurements on carbon samples. Five samples of the same Calgon BPL carbon were analyzed by DSC over a three day period. The carbon samples were tested as received.

##### 3.1.2 Peak Area Measurement

The baselines of the observed DSC curves of carbon samples (shown later in Section 4) were not 'flat' compared to the one normally observed for pure system (e.g. indium metal) or the one shown in Figure 3. Thus, there is a need to determine the shape of the baseline so that the area under the peak on the DSC curve can be measured accurately and consistently. Ehrburger et al (10a) employed a fitting procedure to obtain the baseline for each type of carbon.

In this study, the baseline of the peaks was determined as follows. The first and second derivatives were obtained for the DSC curve, and then all three were plotted together. This can be easily accomplished using the software that comes with the Du Pont 2100 Thermal Analyst. The start of the peak on the DSC curve is defined as the point where the curve acquires a slope greater than zero, and where the slope continues to increase in magnitude. This will be reflected in the first derivative as a sharp rise, while the plot of the second derivative will show an inflection point, i.e. a flat region. The computer software allows one to line up the inflection point from the 2nd derivative, with the corresponding point on the DSC curve. This point on the DSC curve is then used as the peak onset point, i.e. the point where the peak started to 'rise' from the baseline. The end-point of the peak can be determined similarly. A line joining the onset-point and the end-point on the DSC curve is used for purposes of integrating peak areas.

### **3.2 MOISTURE CONTENT DETERMINATION OF CARBON**

It has been mentioned in the Introduction that the DSC has been applied successfully in the determination of moisture content on the carbon. This has been reported earlier in another technical note (9). However, for the purpose of a complete manuscript on the application of DSC to the analysis of carbon, the work on DSC measurement in ref.(9) is reproduced in this report as Annex A.

### **3.3 PREPARATION OF SAMPLES FOR INORGANIC IMPREGNANT ANALYSIS**

Both ASC and ASC/T carbons contain about 8% Cu, 2% Cr, 0.05% Ag, 12% NH<sub>3</sub>, and 10% CO<sub>2</sub>. (ASC/T carbon also contains an extra 2% of triethylenediamine). In order to identify all the peaks on the DSC curve, impregnated carbons containing copper only, chromium only, and copper and chromium only were also studied. These impregnated carbons were prepared in this laboratory, and their properties have been previously reported (2).

### **3.4 PREPARATION OF SAMPLES FOR ORGANIC IMPREGNANT ANALYSIS**

In the experiments involving BPL or ASC carbons containing different TEDA loading levels, the Calgon BPL or ASC carbons were pre-dried at 150°C for three hours inside a 2.2 L vacuum desiccator. The carbon was then cooled to room temperature with the lid on. An accurately weighed amount of TEDA was then added to the carbon sample to obtain desired loading levels of 1-10% (w/w). The container was resealed and a vacuum of 1.33 Pa was applied to the container for one minute. The container plus its contents was then left undisturbed for 2-3 days at 50-60°C. This procedure was developed at DREO and is the subject of a patent application (16).

For carbon samples impregnated with other amines, the same procedure of preparation was employed. These organic amine impregnants include dipropylamine, triethylamine and a combination of dipropylamine and TEDA. All chemicals were obtained from Aldrich Chemical Company Inc., and were used without prior purification.

#### **4.0 RESULTS AND DISCUSSION**

The raw data obtained from DSC were plotted as heat flow (W/g) versus temperature ( $^{\circ}\text{C}$ ). Since a different amount of carbon was placed in the pan each time, the unit of W/g of carbon offered a normalized comparison between different carbon samples. This plot was represented by a curve with a variety of peaks. To compare the peaks of different carbons, the temperature at peak maximum was used as the point of reference.

#### **4.1 ERRORS ASSOCIATED WITH THE DSC INSTRUMENT**

##### **4.1.1 Temperature Measurements**

According to the manufacturer's manual (14), the sensitivity and the temperature reproducibility of the DSC instrument were given as  $6 \mu\text{W}/\text{cm}$  (rms) and  $\pm 0.1^{\circ}\text{C}$  respectively. Similarly, the calorimetric precision (based on metal samples) and the baseline stability were estimated to be 1% and  $400 \mu\text{W}$  respectively.

An estimation of the experimental precision associated with the DSC instrument involving carbon can be carried out by repeated measurements of the same batch, but with different samples of carbon. For this experiment, five samples of the same batch of a Calgon BPL carbon are measured by DSC within 3 days. It has already been reported (9) that the only peak on the DSC curve of a BPL carbon consists of an endotherm corresponding to the desorption of water from the carbon surface occurring at ca  $100^{\circ}\text{C}$ . The results from this experiment are shown in Table 1. As could be observed, the temperature of the peak maximum of the endotherm on the DSC curves from repeated measurements is reproducible within  $\pm 5\%$ .

To ensure the general reproducibility of all the results, a temperature calibration was carried by first, using indium to calibrate the sample thermocouples, and secondly, adjusting the variable resistor in the cell to calibrate the control thermocouple, at least once every two weeks.

**TABLE 1. Experimental Reproducibility of the DSC Instrument  
Using the Endotherm on the DSC Curve of a Calgon  
BPL Carbon**

TRIALS	PEAK MAXIMUM (°C)	AREA UNDER THE CURVE (J/g)
1	128.6	34.9
2	115.4	30.6
3	120.0	30.4
4	130.1	32.5
5	125.1	42.3
AVERAGE	123.8 ± 6.1	34.1 ± 4.9



#### 4.1.2 Area Under The DSC Curve

The area under the exo- or endotherm on the measured DSC curve is proportional to the heat of reaction occurring at that temperature, as shown by equation [4]. Thus this measured quantity is important as the temperature at which the exo- or endotherms occur. For BPL carbon, the endotherm occurring at ca 100°C corresponds to the removal of water from the carbon surface. The heat of reaction measured under this peak area will yield the heat of adsorption of water on carbon, and will indicate how strongly the water is adsorbed on the surface. As shown in Table 1, there exists considerable variation in the measured area under the endotherm for the five carbon samples.

Ehrburger et al (10a) have demonstrated that the equation of the baseline in the temperature range of 100 to 500°C is best expressed in the polynomial form of  $(a + bT + cT^2 + dT^3)$ , where T is the temperature and the coefficients a, b, c, and d can be determined experimentally for each type of carbon. In this way, Ehrburger et al.(10a) reported an experimental reproducibility of the DSC as  $\pm 1.5$  J/g.

As shown in Table 1, the calculated standard deviation for area measurement, and thus the heat of reaction is about  $\pm 15\%$ . This is due to the difficulty in locating the inflection point on the second derivative of the DSC curve. However, it should be noted that this is not a resolution problem. A slower heating rate of 10°C/min did not improve the resolution, and the identification of the peak onset point (and thus the peak baseline) was not refined.

#### 4.1.3 Consistency of the DSC Curves

DSC curves were obtained for Calgon ASC carbons from three different lots. They are Lot No. 1048 (which is more than 10 years old), Lot No. 1715 (which is about 2 years old) and Lot No. 1746 (which is about one year old). All carbons contain similar amounts of copper (6-8%), chromium (2%) and silver (0.05%). The only difference was the amount of water present. It is to be expected that the ASC carbon from Lot No. 1048 will contain more water than the other two. Figure 4 displays the difference between all three carbons and Table 2 lists the temperatures and peak areas corresponding to the water removal (endotherm); the exothermic peak corresponds to the reaction between the metal impregnants and the carbon surface at ca 270°C. The designation of the enthalpic changes will be explained later in Section 4.2.

DSC measurements were run at least twice for each lot. For the endotherm peak corresponding to water removal, the average standard deviation for the temperature maximum is about 10%, while it is about 22% for the area under the DSC curves. The major

**TABLE 2: Consistency of DSC Curves (As Demonstrated by Using Different Lots of Calgon ASC Carbon.**

ASC CARBON LOT #	Endothermic Peak		Exothermic Peak	
	PEAK MAX (°C)	AREA (J/g)	PEAK MAX ( °C)	AREA (J/g)
1746	145.5	10.2	271.0	67.2
	117.7	6.2	266.0	47.6
	116.6	7.4	264.4	51.1
Average	126.6 ± 16.4	8.0 ± 2.1	267.1 ± 3.4	55.3 ± 10.5
1715	114.1	30.3	264.7	75.0
	130.5	27.6	261.5	63.7
	122.3 ± 11.6	28.9 ± 1.9	263.1 ± 2.3	69.3 ± 8.0
Average	122.3 ± 11.6	28.9 ± 1.9	263.1 ± 2.3	69.3 ± 8.0
1048	129.1	57.1	265.9	67.0
	135.5	65.4	269.2	81.0
	114.5	32.1	262.7	56.7
Average	126.4 ± 10.8	51.5 ± 17.3	265.9 ± 3.3	68.2 ± 12.2

feature is, of course, the large size of the endotherm for Lot No. 1048, indicating the large amount of water. The temperature of the exotherm corresponding to the reaction between the metal impregnants and the carbon surface has an average standard deviation of 1%, but it is about 16% for the peak area under the exotherm. This large standard deviation seems to indicate that for most purposes, DSC is best employed as a qualitative tool. Although the DSC curves for Lot Nos. 1715 and 1746 appeared similar, the areas measured under the curves (for the water endotherm) were quite different. As was pointed out earlier in Section 3.1.2, the peak area measurement depends largely on where the onset and the end-point of the peak are, and also on the shape of the baseline. Thus two similar DSC curves may have different areas under the peaks.

#### 4.2 TYPICAL DSC CURVES FOR CALGON CARBONS

Typical DSC curves for Calgon BPL, ASC and ASC/T carbons are shown in Figure 5. For all three activated carbons, the only common feature on the DSC curve was the first endotherm observed at ca 60-160°C. This endothermic peak corresponds to the desorption of water from the carbon surface (9). The temperature of this endotherm appears to be dependent on both the type of carbon and the amount of water on the carbon surface. It appears that while the endotherm has a peak maximum at around 100°C for BPL carbon, it occurs at ca 125°C for both ASC and ASC/T carbons. Furthermore, there is a shift to higher temperature as the amount of water on the carbon surface increases (9). The explanation for this observation has been given in Annex A.

For the Calgon BPL carbon, the DSC curve showed a constant decline with a slope of  $-9.2 \times 10^{-4}$  W/g/°C from 100°C to 600°C. This is attributed to a continuous heating of the carbon (surface and lattice) releasing CO, CO<sub>2</sub>, NH<sub>3</sub> and H<sub>2</sub>O from the sample. This observation was less obvious for Calgon ASC and ASC/T carbons, and is probably obscured by other enthalpic changes on the DSC curve because of the complexity of the surface reactions occurring on these carbons at various temperatures.

The DSC curve of Calgon ASC carbon showed an exotherm at ca 270°C, a shoulder at ca 300°C and a broad exotherm at ca 500°C. These exotherms are believed to arise from the reactions of the impregnants (copper, chromium and silver) with the carbon surface. The assignment of these enthalpic changes is detailed in Section 4.3.

For the Calgon ASC/T carbon, the DSC curve showed two exotherms at ca 240°C and 340°C. The exotherms were observed at temperatures which were quite different from those observed for ASC carbon. If TEDA is adsorbed on the carbon surface as a distinct species, one would have expected a DSC curve containing four

exotherms, i.e. three exotherms at 270°C, 300°C and 500°C, similar to the DSC curve of an ASC carbon, and a fourth one, corresponding to TEDA. Obviously, the 'expected' DSC curve is quite different from what was observed. The interaction of TEDA with the carbon surface, and with other impregnants may be more complicated than is expected. The assignment of the exotherms will be discussed in Section 4.4.

In summary, the first endotherm observed for BPL, ASC, and ASC/T carbons was due to the water removal from the carbon surface. In the case of ASC and ASC/T carbons, the observed DSC curves are quite different from each other, and the interpretation may be quite complicated.

#### 4.3 INORGANIC IMPREGNANTS ON ASC CARBON

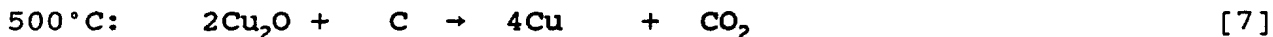
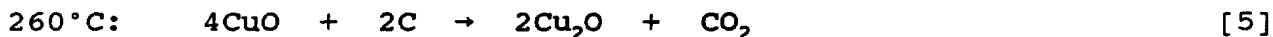
The DSC curve of the Calgon ASC carbon contains as observed above, an endotherm at 100 to 120°C, an exotherm at ca 270°C, a shoulder at ca 300°C and a broad exotherm at ca 500°C. Since the endotherm has been assigned to the water desorbed from the carbon surface, the other peaks must have arisen from the metal impregnants.

The impregnation formulation of the Calgon ASC carbon contains the following constituents in water (1,2):

Basic Copper Carbonate	$\text{CuCO}_3 \cdot \text{Cu}(\text{OH})_2$
Chromium (VI) Oxide	$\text{CrO}_3$
Ammonium Hydroxide	$\text{NH}_4\text{OH}$
Ammonium Carbonate	$(\text{NH}_4)_2\text{CO}_3$
Silver Nitrate	$\text{AgNO}_3$

This formulation in proper proportions will produce an impregnated carbon containing about 6-8% copper, 1-3% chromium, 0.05% silver, 10% carbon dioxide and 12% ammonia (1,2).

With reference to the work by Ehrburger (10), and the work carried out in this laboratory (to be detailed later), it is believed that the observed exotherms for ASC carbon shown in Figure 4 are due to the following reactions on the carbon surface:



In order to understand and designate the reactions occurring on the carbon surface, DSC measurements were made on BPL carbon which had been impregnated with one impregnant only (the experimental procedure has been described in Section 3.3). Typical examples are shown in Figure 6. For example, the DSC thermogram of

a BPL carbon impregnated with copper only showed three enthalpic changes only: one endotherm at ca 120°C for water removal, and exotherms at ca 285°C and 507°C, as shown in Figure 6. The main impregnant used is  $\text{CuCO}_3 \cdot \text{Cu}(\text{OH})_2$ , basic copper carbonate, which decomposes at 200°C to give  $\text{CuO}$ . (The DSC thermogram of a BPL carbon impregnated with a mixture of ammonium hydroxide and ammonium carbonate is the same as that of plain BPL carbon. Thus it is assumed that ammonia and carbon dioxide do not react with the carbon surface to any extent.) Thus the active species on the carbon surface is likely to be  $\text{CuO}$  rather than  $\text{Cu}_2\text{O}$ . The reaction between  $\text{CuO}$  and C is then believed to be the reaction occurring at 260°C. At 507°C, the exotherm is believed to arise from the reaction between  $\text{Cu}_2\text{O}$  and C.

It should be stressed that there was indeed a reaction between the impregnants and the carbon. The DSC curve of pure basic copper carbonate, shown in Figure 7, contains only one sharp endotherm at 272.5°C, which is in contrast to that shown in Figure 6.

The DSC curve for the activated carbon impregnated with  $\text{CrO}_3$  only, shown in Figure 6, contains one major exotherm at 304°C. It is believed that the reaction between  $\text{CrO}_3$  and C is more likely than the one between  $\text{Cr}_2\text{O}_3$  and C. (The reaction between  $\text{Cr}_2\text{O}_3$  and C, yielding Cr and  $\text{CO}_2$  is believed to occur at much higher temperatures, probably around 800°C (10).) The DSC curve of pure  $\text{CrO}_3$ , shown in Figure 8 is distinctly different from that shown in Figure 6, indicating that a reaction did indeed occur between  $\text{CrO}_3$  and the carbon surface. The DSC of a BPL carbon impregnated with Cr(III) (in the form of chromium nitrate) showed no feature, except the water endotherm, as shown in Figure 6.

Theoretically, adding the DSC curve of a copper-only impregnated carbon to the DSC curve of a chromium-only impregnated carbon would yield a composite DSC curve very close to the DSC curve of the Calgon ASC carbon. This is indeed the case, as the composite curve shows exotherms at 285, 303 and 507°C, very close to that of a Calgon ASC carbon. Figure 9 showed the DSC curve of a BPL carbon impregnated with copper and chromium together, which resembles quite closely with that of Calgon ASC carbon. The DSC curve of a mixture of copper and silver (about 0.2% by weight) is quite different from the DSC curve of Calgon ASC carbon. The shoulder of this DSC curve at 254°C is attributed to the presence of silver. This shoulder is not apparent on the DSC curve of Calgon ASC carbon because the silver content is small (ca. 0.05% by weight). The copper exotherms occurring at 270° and 507°C for ASC carbon have been shifted to 293°C and 497°C respectively. The reason for this is not immediately obvious.

It has been pointed out by various authors (17,18) that the active impregnant on the ASC carbon is a copper chromate, i.e.  $\text{CuCrO}_4$  or  $\text{Cu}(\text{NH}_4)\text{CrO}_4$  type of species, rather than simpler species like  $\text{Cu}^{++}$ ,  $\text{CuO}$  or  $\text{CrO}_3$  etc as claimed by others (6,19). The present

observation showed that the DSC curve for an ASC carbon is a composite of the DSC for Cu-impregnated carbon superimposed on the DSC curve of a Cr(VI)-impregnated carbon. However, it does not rule out the presence of copper chromate on the carbon surface.

#### 4.4 ORGANIC IMPREGNANTS (TEDA) ON CARBON

##### 4.4.1 DSC Thermograms of BPL and ASC Carbons Impregnated with TEDA

One might naively expect that a DSC thermogram for the ASC/T carbon would consist of four major exotherms: three due to copper and chromium at 270, 300 and 500°C (as shown above in Sections 4.2 and 4.3), and one exotherm for TEDA, if the impregnants are located on the carbon surface as distinct species. However, this is not the case here. The DSC curve of ASC/T shown in Figure 5 contained two major exotherms at 240 and 340°C and a broad smaller peak at 500°C.

To understand this DSC thermogram of ASC/T carbon better, DSC measurement was also carried out for specially TEDA-impregnated carbons. Two carbons, one a Calgon BPL and the other, a Calgon ASC carbon were impregnated with TEDA at 10% (w/w) loading level, and the DSC thermograms were obtained. The DSC curves in Figure 10 are quite different. For BPL/TEDA carbon, the exotherms occur at ca 264°C and 340°C while the exotherms occur at ca 225°C and 272°C for the ASC/TEDA carbon.

TEDA has a melting point at 158-160°C. If there exists no interaction between TEDA and the carbon surface, the expected DSC curve for a BPL carbon impregnated with TEDA would contain an endotherm around 160°C, indicating the melting of TEDA. However, two exotherms appear at temperatures beyond the melting point of TEDA. Exothermal peaks indicate that heat is being given off, and are usually associated with a chemical reaction. It seems that TEDA is reacting with the BPL carbon surface. One plausible explanation may be attributed to the reaction between triethylenediamine with the C-OH, C=O, or C-H species on the carbon surface, forming amide or nitrile type products.

It is well known that amines (especially tertiary amines) are oxidized easily to amine oxides,  $R_3N^+-O^-$  (20). Since the DSC was run under dry nitrogen, it is anticipated that the source of oxygen comes from the carbon surface, e.g. the C-OH, or C=O groups. Furthermore, it has been shown (20) that amine oxide containing  $\beta$ -hydrogen undergoes decomposition to form an alkene and a derivative of hydroxylamine (the Cope elimination) at high temperature. The observed DSC exotherms may then be explained as consisting of two consecutive reactions: first, a reaction of TEDA with the surface species (such as C-OH, C=O etc) at around 260°C, and then the product of this reaction undergoes further reaction at higher

temperature (ca 340°C). This conjecture may be substantiated if suitable gas chromatography-mass spectrometry equipment is connected at the effluent side of the DSC to collect all gaseous and air-borne reaction products. This addition is being set up at this laboratory, and the results will be reported shortly.

The DSC curve of the ASC carbon impregnated with 10% TEDA appeared sufficiently different from the DSC of BPL carbon impregnated with 10% TEDA that one cannot simply conclude that the observed exotherms have shifted. The picture of the adsorption of TEDA on ASC carbon would be quite different from that on the BPL carbon. While the active sites on both carbons may be the same, the metals on the ASC carbon will exist essentially in the ionic form (i.e. as electron-deficient species), which will in turn create a stronger attraction to the lone pair of electrons on the TEDA molecule. Thus there will be a stronger tendency to find the TEDA molecules adsorbed in close proximity to the metal impregnants. It is then very possible to find a copper-TEDA or chromium-TEDA type of complex on the ASC carbon impregnated with TEDA (21).

Based on the observed DSC curve, it is conjectured that the exotherms occurring at 225 and 272°C arise mainly from the chemical reactions between TEDA and the carbon surface, with a portion due to the reactions between the Cu-TEDA and Cr-TEDA with the carbon surface. Furthermore, it may be suggested that the exotherm at lower temperature (at 225°C) arises from the reactions between the Cu-TEDA and Cr-TEDA with the carbon surface, while the higher-temperature exotherm indicates the reaction between TEDA and the carbon surface.

#### **4.4.2 Quantitative Analysis of TEDA Content on Carbon by DSC Measurements**

It has been shown in a previous report (9) that a linear relationship exists between the area under the DSC curves and the amount of moisture on the carbon surface (reproduced in this report as Annex A). It is imperative to see if a similar relationship exists between the area under the DSC curve and the amount of TEDA loaded on the ASC carbon. (This experiment was not carried out for BPL carbon because TEDA-impregnated BPL carbon has no practical value). A batch of Calgon ASC carbon (Lot No. 1715) was impregnated with 1-10% (w/w) loading levels of TEDA. Figure 11 shows the DSC curves of some of the selected ASC/TEDA carbons. It is evident that as the amount of TEDA on the carbon increases, there are noticeable shifts in the temperatures where the two exothermic peaks occur. This trend is shown in Figure 12, where the peak maximum temperatures were plotted against the percentage loading levels of TEDA on the ASC carbon. The data are listed in Table 3.

**TABLE 3: Peak Areas from DSC Curves of ASC/TEDA Carbon Containing Different Loading Levels of TEDA Produced in this Laboratory**

% TEDA LOADING	PEAK 1		PEAK 2		PEAK 3	
	PEAK MAX (°C)	AREA (J/g)	PEAK MAX (°C)	AREA (J/g)	PEAK MAX (°C)	AREA (J/g)
0	117.7	6.2	266.0	47.6	-	-
0	116.6	7.4	264.4	51.1	-	-
1	126.0	28.9	259.2	69.3	339.4	0.5
1	137.6	7.6	240.9	61.4	339.8	2.5
1.5*	126.0	26.5	236.9	81.0	383.7	2.2
1.63	138.2	16.0	263.9	61.2	343.6	0.6
1.63**	135.8	12.3	260.2	52.3	340.2	0.6
2	125.7	20.9	237.4	--	332.0	0.3
2	126.7	20.7	235.2	--	327.2	0.7
2.66	135.7	13.7	236.0	68.4	345.2	4.7
3	138.8	24.5	239.8	53.6	341.8	2.4
3.73	126.0	11.9	230.5	72.2	322.1	10.2
3.73**	128.2	12.1	231.3	72.7	327.2	10.7
4	125.4	9.0	232.7	54.9	333.5	4.6
4	132.9	31.3	229.7	66.3	303.6	18.0
4.68	130.1	11.4	233.3	55.1	306.5	6.9
6	126.5	9.2	228.5	50.3	284.2	2.4
7.82	116.7	10.1	261.5	37.6	265.0	6.7
10	121.3	7.3	223.0	41.2	272.6	8.5
10**	125.8	16.0	227.1	66.6	287.6	16.9

The base carbon used is a Calgon ASC carbon Lot #1746.

\* This carbon is a Calgon ASC/T Lot #947

\*\* Indicates repeated measurements of the same lot but different samples of carbon.

- Indicates unmeasurable peak area.



For the exotherm occurring at ca 220°C (labelled as Peak 2; the Peak 1, an endotherm, is identified as the water desorption), the temperature at which it occurred remained quite constant. However, this is not the case for the exotherm occurring at higher temperature (labelled as Peak 3). There is a continual shift to lower temperatures as the loading level of TEDA increases. The regression coefficient ( $R^2$ ) for this linear relationship was determined to be 0.73. One possible explanation for this is that there is a poor thermal contact between the adsorbed TEDA causing this reaction (and thus giving rise to this exotherm) inside the carbon sample and the constantan disk. Thus the heat generated from the chemical reaction was not observed immediately for the lower loading levels of TEDA. However, as the amount of TEDA increases inside the carbon sample, the thermal contact between TEDA and carbon improves. Thus the observed temperature at which the reaction occurs will decrease.

A plot of the total area under the two exotherms (i.e. Peaks 2 and 3) versus the amount of TEDA loading is shown in Figure 13. The relationship appeared to be linear with a regression coefficient ( $R^2$ ) determined to be 0.85. It is suggested that the total area under the exotherms on the DSC curve may be used as a quantitative estimate of the percentage loading of level of TEDA on ASC carbon.

#### 4.5 OTHER ORGANIC IMPREGNANTS

DSC measurements were extended to Calgon ASC carbon impregnated with other amine compounds. The results are summarized in Table 4. Figure 14 shows the DSC curves of ASC carbon (Calgon Lot No. 1746) impregnated with triethylamine (7% w/w) and dipropylamine (5% w/w) and a ASC/T carbon (Calgon Lot No. 947) impregnated with dipropylamine (5% w/w). These DSC curves are distinct, and quite different from that for the Calgon ASC/T carbon shown earlier. For example, the DSC curve for the ASC/T carbon impregnated with 5% dipropylamine yields exotherms at 208 and 269°C, quite different from the major peaks at 240 and 340°C observed for Calgon ASC/T carbon shown in Figure 5. Actually, the DSC curve for this carbon resembles more closely the DSC curve of the ASC carbon containing 5% dipropylamine, than that of the Calgon ASC/T carbon. One explanation is that, since dipropylamine is more abundant on the carbon surface (at 5% w/w), the exotherms arising from the reaction of this impregnant would obscure that from the reactions between TEDA and the carbon surface. This would have to be confirmed by establishing a large database of DSC measurement of amine-impregnated carbons.

The most interesting DSC curve observed so far was that of 7% (w/w) triethylamine impregnated on ASC carbon. The baseline of this DSC curve is above zero, unlike the continually declining DSC curves shown for other activated carbons. Obviously the reactions

TABLE 4: Peak Areas From DSC Traces of Carbon with Various Organic Impregnants

ASC/A	PEAK 1		PEAK 2		PEAK 3		PEAK 4	
	PEAK MAX (°C)	AREA (J/g)	PEAK MAX (°C)	AREA (J/g)	PEAK MAX (°C)	AREA (J/g)	PEAK MAX (°C)	AREA (J/g)
Calgon Lot # 937YB	84.6	12.9	---	---	---	---	---	---
Calgon Lot # ASC 1746	117.7	6.2	265.9	47.6	---	---	---	---
Calgon Lot # ASC/T 947	125.9	26.5	236.9	81.0	383.7	2.2	---	---
Calgon ASC* + 7% TEA	127.8	26.7	212.3	34.3	312.8	5.1	---	---
Calgon ASC + 5% DPA	115.6	58.7	198.2	39.8	280.8	15.2	498.8	7.3
Calgon ASC + 7% DPA	118.1	41.1	203.5	30.5	292.6	13.7	---	---
Calgon ASC/T** + 7% DPA	111.3	36.3	205.8	20.7	275.3	17.1	---	---

NOTE: TEA = Triethylamine  
DPA = Dipropylamine

\* The base carbon is Calgon ASC carbon Lot # 1746.

\*\* The base carbon is Calgon ASC/T carbon Lot # 947 (containing 2% TEDA).

occurring between the carbon surface and the impregnants (the triethylamine and the metals) are quite different from those of other amine impregnants studied so far.

#### 4.6 IMPREGNATED CARBONS FROM OTHER SOURCES

So far, only Calgon carbons of the types BPL, ASC, and ASC/T have been investigated. In order to complete this study, and to completely assess the analytical capabilities of the DSC, carbons from other sources were also analyzed.

Figure 15 shows the DSC curve of Calgon ASC/T carbon, Norit ASC carbon and Sutcliffe-Speakman ASC/T carbon. It is obvious that the DSC curves for all three carbons are quite different. The DSC curve of the Norit ASC carbon is almost an exact duplicate of the DSC curve of the Calgon ASC carbon. This indicates that both carbons probably have the same precursor (i.e. are coal-based), and that the impregnation formula and procedure are probably very similar also. For the ASC/T type carbons, there is more variation between the two manufacturers of Calgon and Sutcliffe-Speakman. While the low-temperature exotherm for both carbons occurred at similar temperatures, the high-temperature one occurred at higher temperature (ca 400°C) for the Sutcliffe-Speakman carbon. This is attributed to different precursors and/or different impregnation procedures. It is believed that Sutcliffe-Speakman is currently using coconut-shell as the carbon precursor (instead of the New Zealand coal) (22). Table 5 compared peak maximum temperature and the area under the exothermic peaks for the Calgon, Norit and Sutcliffe-Speakman carbons. As shown in the table, the positions of the exothermic peaks vary with the type and concentration of the impregnants used in the preparation of the carbon.

#### 5.0 CONCLUSIONS

It has been demonstrated in this report that Differential Scanning Calorimetry (DSC) can be used as an analytical tool for the characterization of activated carbons. With caution, DSC can also be employed in the quantitative determination of the amount of TEDA present on ASC/T carbon. This caution is necessary because of the inherent uncertainty of  $\pm 15\%$  associated with the DSC measurements. As a qualitative tool, DSC can be used to distinguish activated carbons containing different impregnants, and from various manufacturers.

TABLE 5: Peak Areas From DSC Curves of Carbons from Various Sources

TYPE OF CARBON	PEAK 1		PEAK 2		PEAK 3	
	PEAK MAX (°C)	AREA (J/g)	PEAK MAX (°C)	AREA (J/g)	PEAK MAX (°C)	AREA (J/g)
Calgon ASC Lot # 1746	117.7	6.2	266.0	47.6	--	--
Calgon ASC/T Lot # 947	125.9	26.5	236.9	81.0	383.7	2.2
Calgon ASC/T Lot # 121 T	140.3	39.7	235.5	57.4	349.2	5.8
Sutcliffe-Speakman Lot # CN521	113.7	27.3	246.1	44.3	337.4	1.8
NORIT ASC Lot # RGG0.8	140.2 134.3	37.9 51.2	276.8 271.8	46.6 60.6	-- --	-- --

**6.0 REFERENCES**

1. R.J. Grabenstetter and F.E. Blancet, Summary Technical Report of Division 10. National Defence research Committee. Vol.1: Military Problems with Aerosols and Non-Persistent Gases. Chapter 4 - Impregnation of Charcoal (1946).
2. S.H.C. Liang, B.H. Harrison, R.T. Poirier, B. Zanette and J.G. Pagotto, DREO Report No. 983 (1988).
3. S.H.C. Liang, unpublished results.
4. S.H.C. Liang, B.H. Harrison and J.G. Pagotto, DREO Report No. 973 (1987).
5. J.L. Hammarstrom and A. Sacco Jr., CRDEC-SP-84014, Proc. 1983 US Army CRDEC Sci. Conf. on Chemical Defence Research 563-9 (1984).
6. V.R. Deitz, J.N. Robinson and E.J. Poziomek, Carbon 13, 181 (1975).
7. J.A. Rossin, CRDEC Report CRDEC-TR-068, Aberdeen Proving Ground, MD, USA (1989).
8. N.S. McIntyre, G.R. Mount, T.C. Lipson, R. Humphrey, B. Harrison, S. Liang and J. Pagotto, Carbon 29, 1071 (1991).
9. L.E. Cameron and S.H.C. Liang, DREO Technical Note 91-25 (1991).
10. See for example: (a) P. Ehrburger, J. LaHaye, P. Dziedzic and R. Fangeat, Carbon 29, 297 (1991); (b) P. Ehrburger, J. Dentzer, J. LaHaye, P. Dziedzic and R. Fangeat, Carbon 28, 113 (1990); and references therein.
11. C. Duval, Inorganic Thermogravimetric Analysis, 2nd edition, Elsevier, Amsterdam (1963).
12. J.L. McNaughton and C.T. Mortimer, Differential Scanning Calorimetry, Intern. Rev. Sci. Phys. Chem. Ser. 2, vol 10, p. 1-44, Butterworth, London (1975).
13. W.W. Wendlandt, Thermal Methods of Analysis, 3rd edition, Wiley-Interscience, New York (1985).
14. Operator's Manual of Du Pont Thermal Analyst 2100, Version 8.1 (1989); Operator's Manual for Du Pont Instruments Differential Scanning Calorimeter 910, (1985).

15. Thermal Characterization of Polymeric Materials (E. A. Turi, ed.), Chapter 1, Academic Press, Toronto (1981).
16. S.H.C Liang, B.H. Harrison and J.G. Pagotto, Canadian Patent Application Serial No. 2015810 (1990); European Patent Application Serial No. 91106863.3 (1991); US Patent Application Serial No. 07/691,323 (1991).
17. P.N. Krishnan, A. Birenzvigge, E.D. Poziomek, V.R. Deitz and S.A. Katz, CRDEC-SP-88013, Proc. 1987 US Army CRDEC Sci. Conf. on Chemical Defence Research, 409-413 (1988).
18. J.L. Hammarstrom and A. Sacco Jr., J. Catal. 112, 267 (1988).
19. R. Berg, A.H. Gulbrandsen and G.A. Neefjes, Rev. Port. Quim 19 (1-4) 378 (1977).
20. See for example: A.L. Ternay Jr. Contemporary Organic Chemistry, Chapter 21, W.B. Saunders Co. Toronto (1979).
21. Dr. David T. Doughty, Calgon Carbon Corporation, private communication, October 1991.
22. Dr. Alan Grint, Sutcliffe-Speakman Carbons Ltd., private communication, October 1991.
23. See for example: S.S. Barton and J. Koresh, J. Chem. Soc., Faraday Soc. I, 79, 1157 (1983).

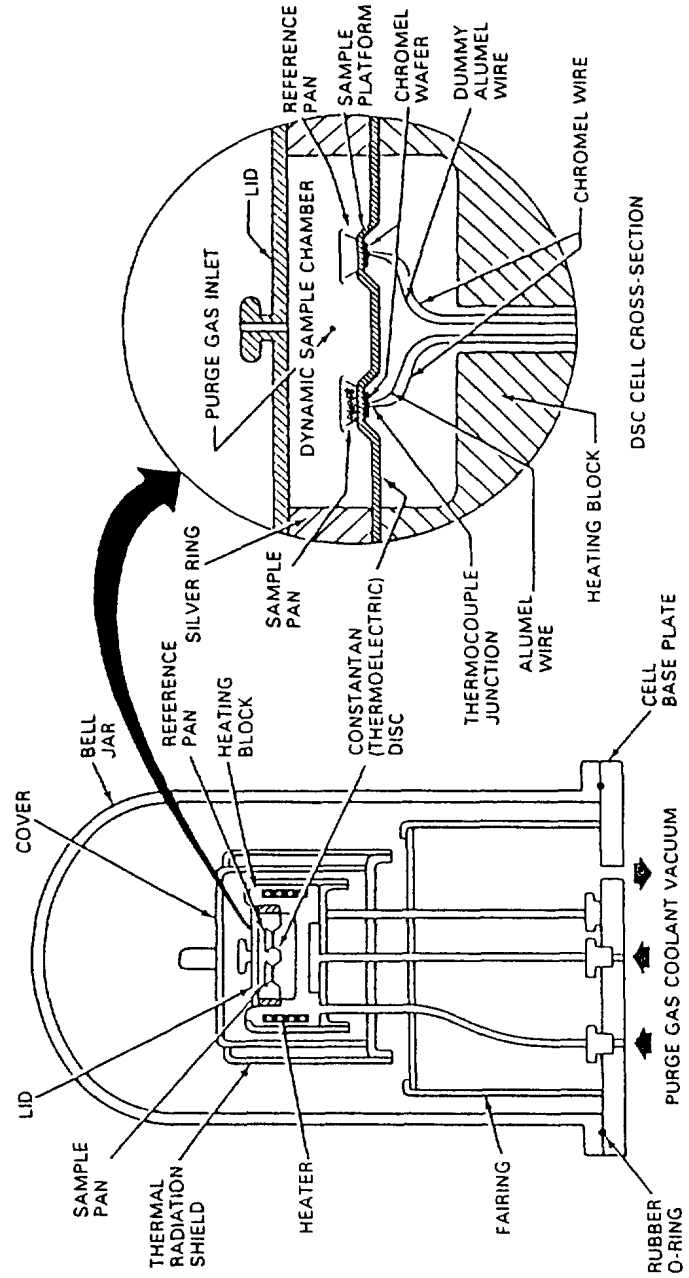


Figure 1: The Schematic of a DuPont 910 DSC Cell.

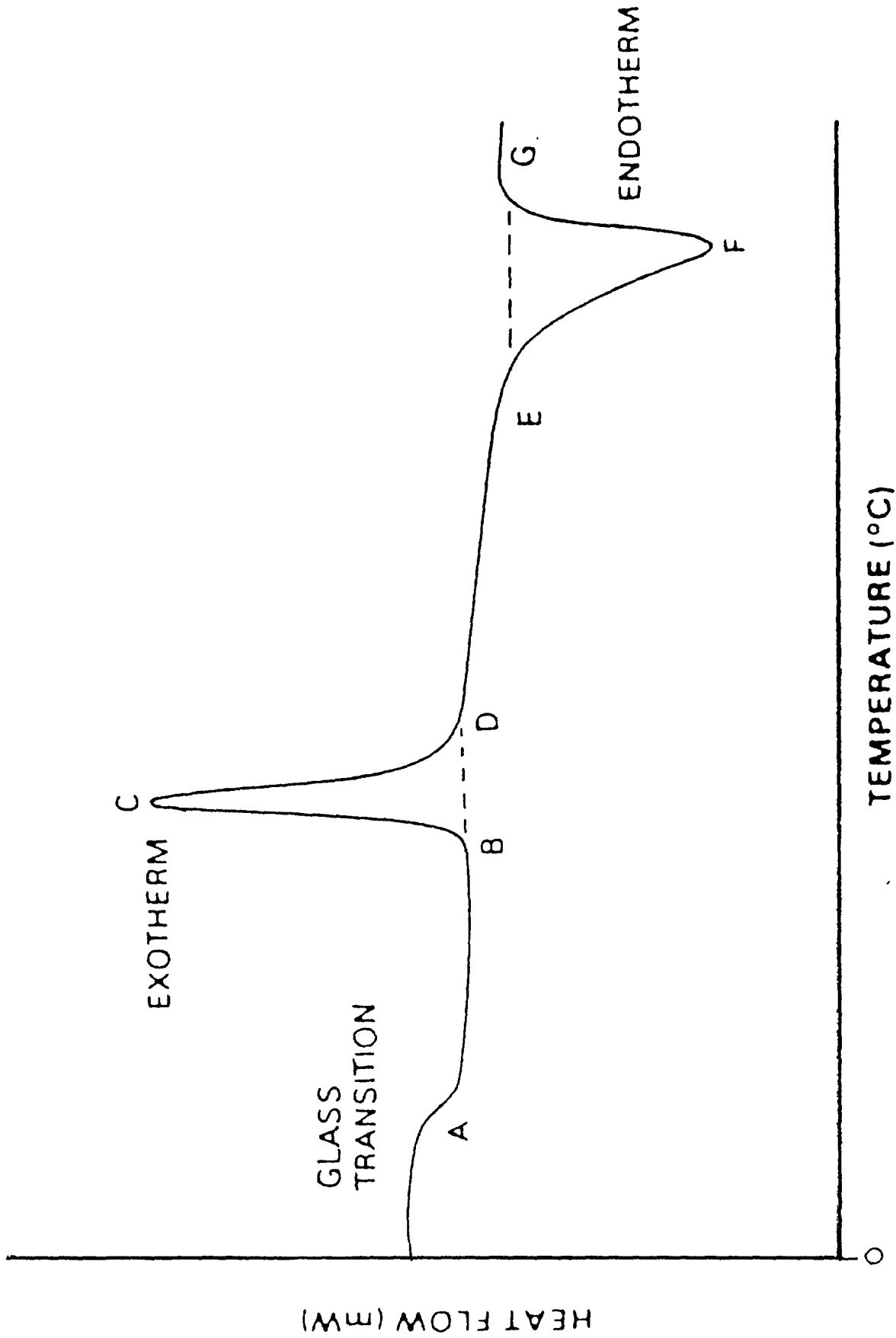


Figure 2: A Typical DSC Curve



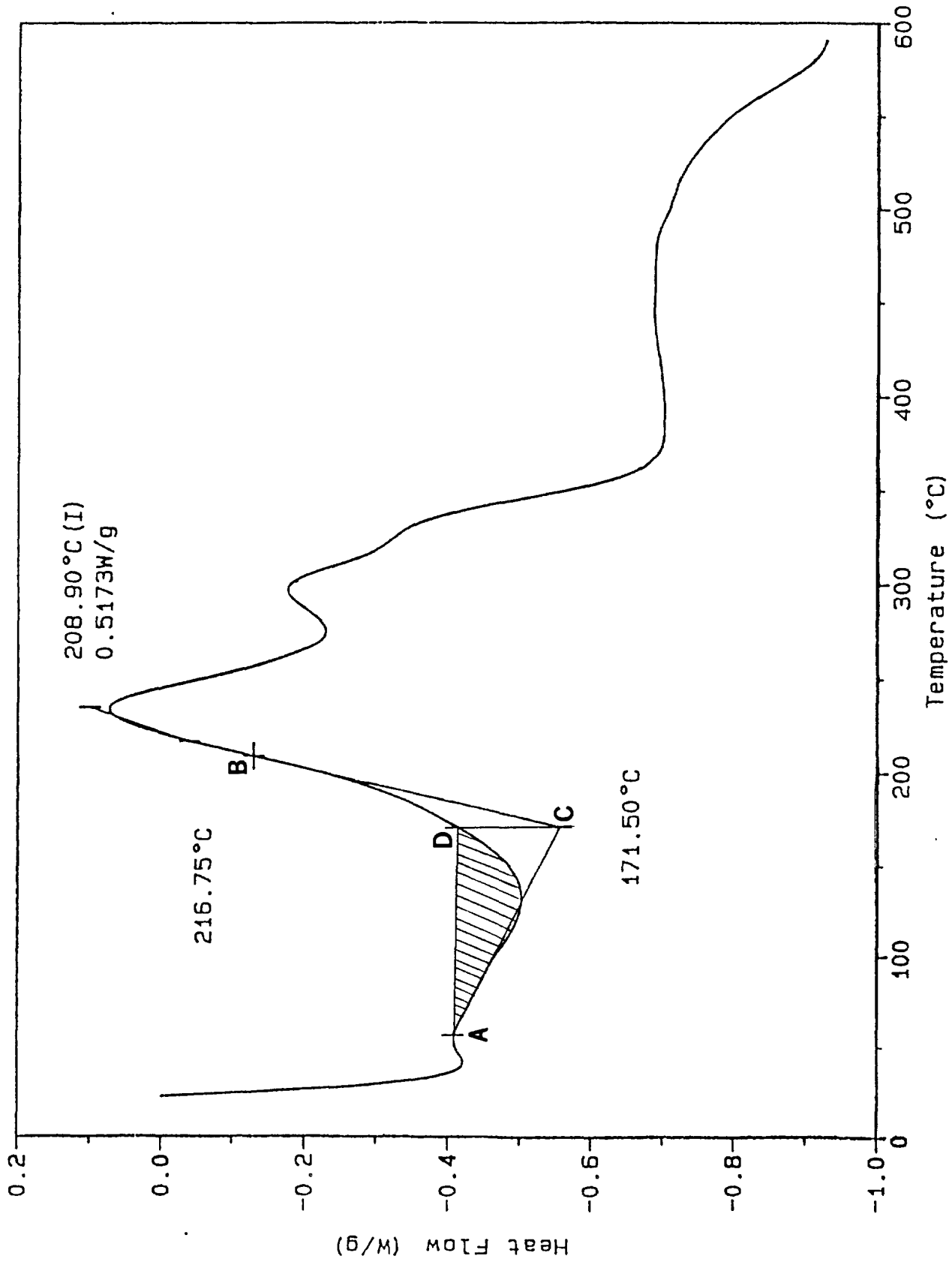


Figure 3: A Simulated DSC Curve Demonstrating How the Area Under the Curve is Determined

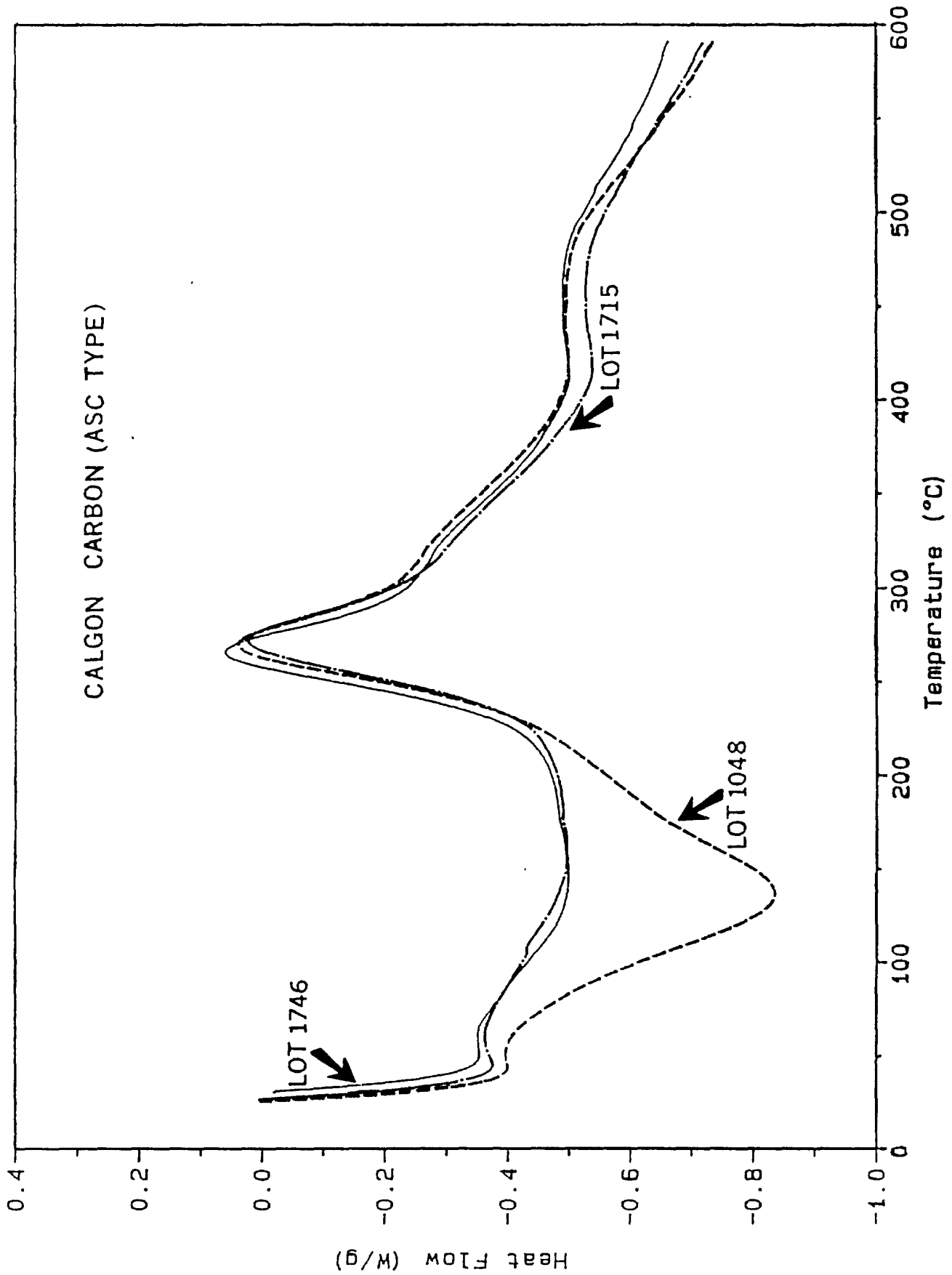


Figure 4: DSC Curves of Three Calgon ASC-types Carbons  
Demonstrating the Consistency of the DSC Measurements

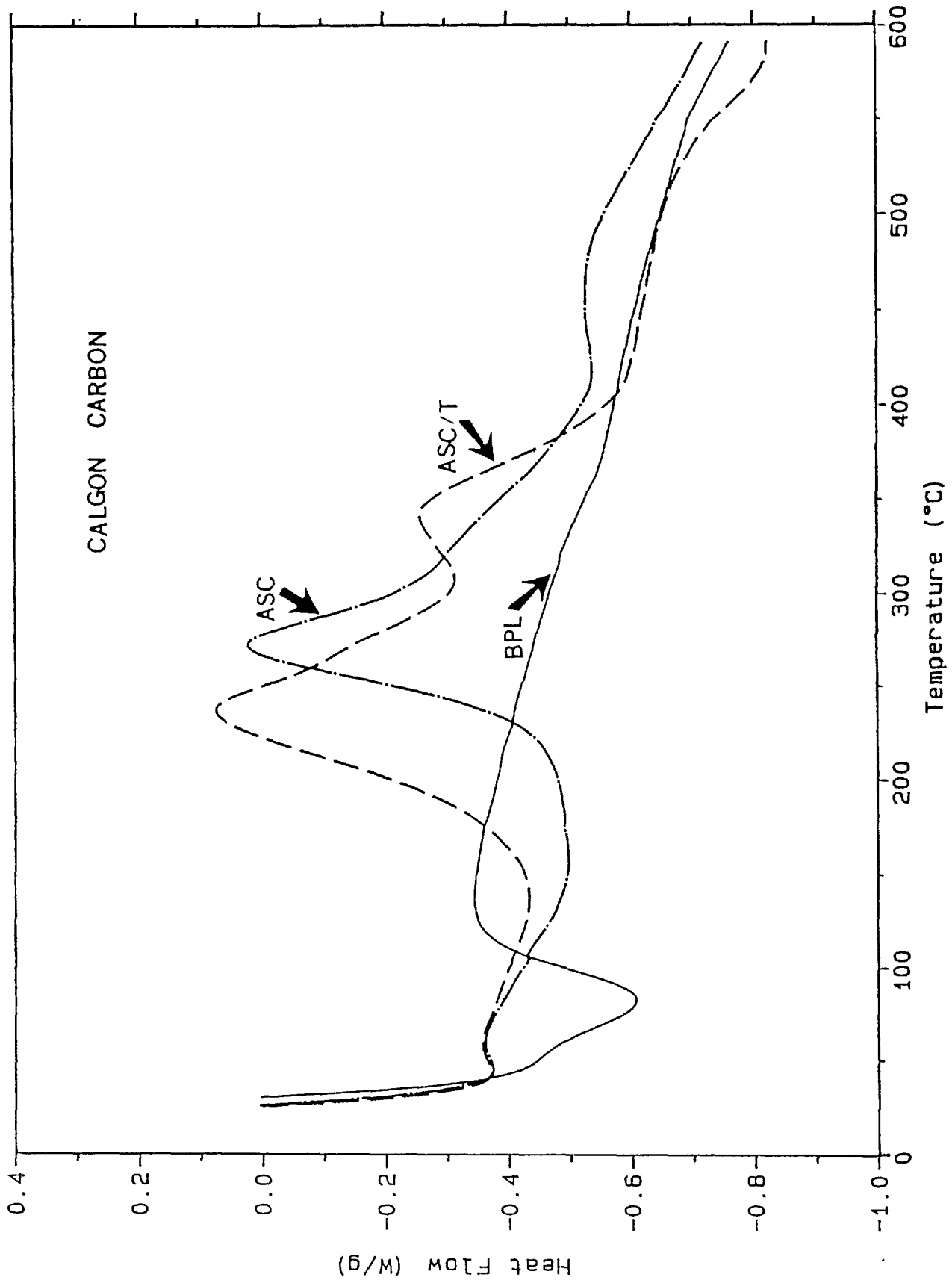


Figure 5: Typical DSC Curves of Calgon BPL, ASC AND ASC/T Carbons

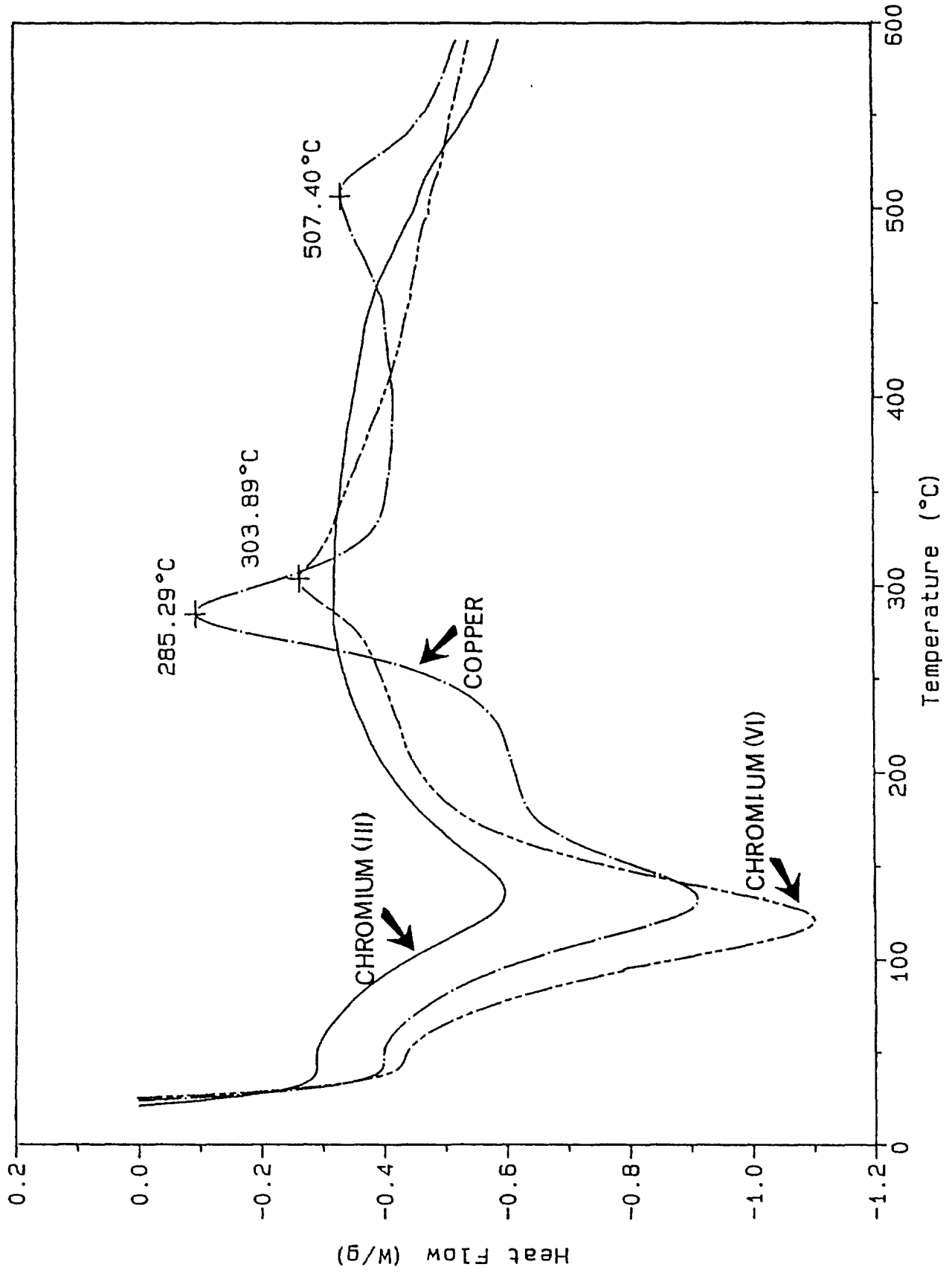


Figure 6: DSC Curves of Several One-Impregnant ASC-Type Carbons

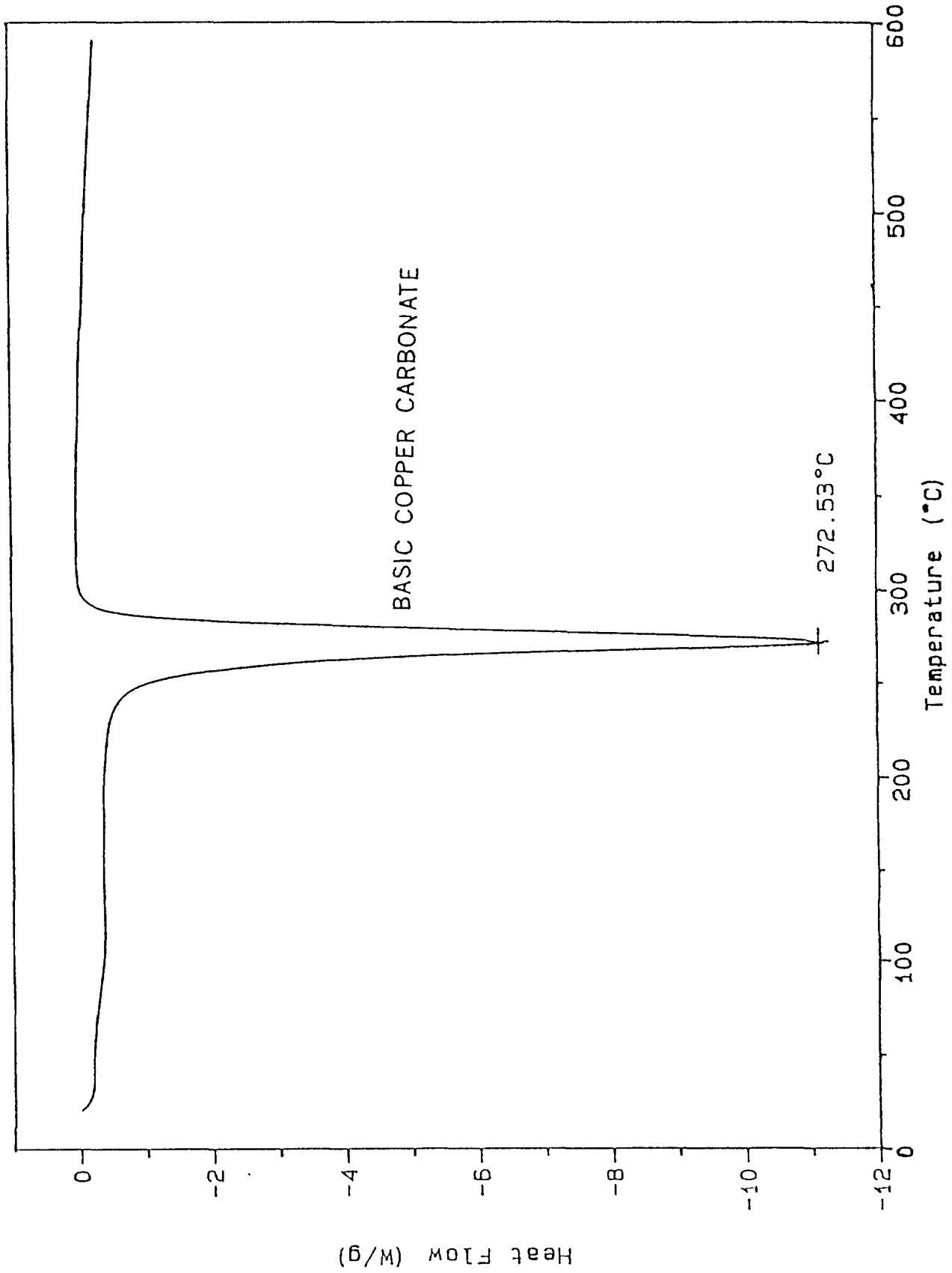


Figure 7: DSC Curve of a Crystal of Basic Copper Carbonate

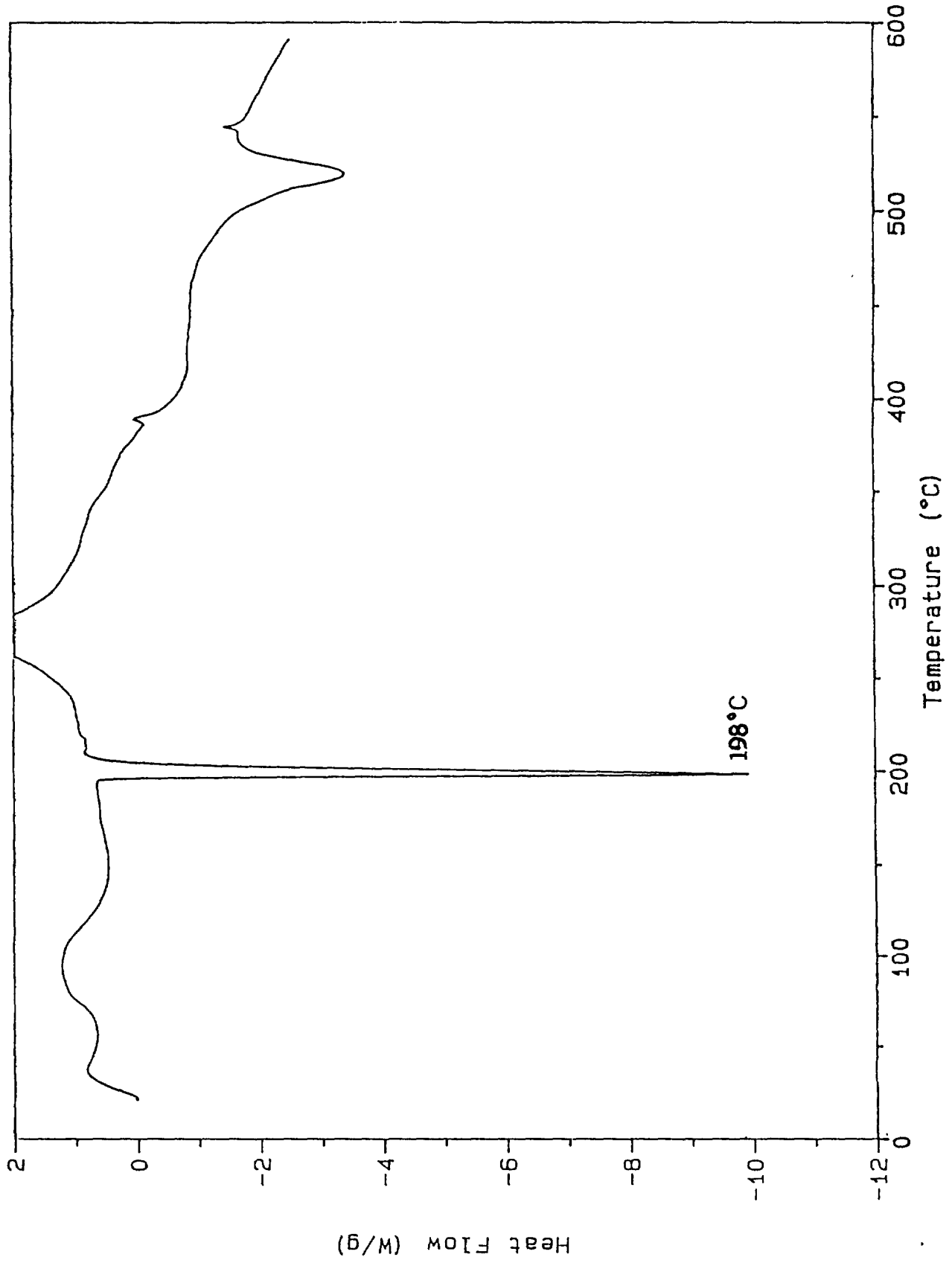


Figure 8: DSC Curve of a Crystal of  $\text{CrO}_3$

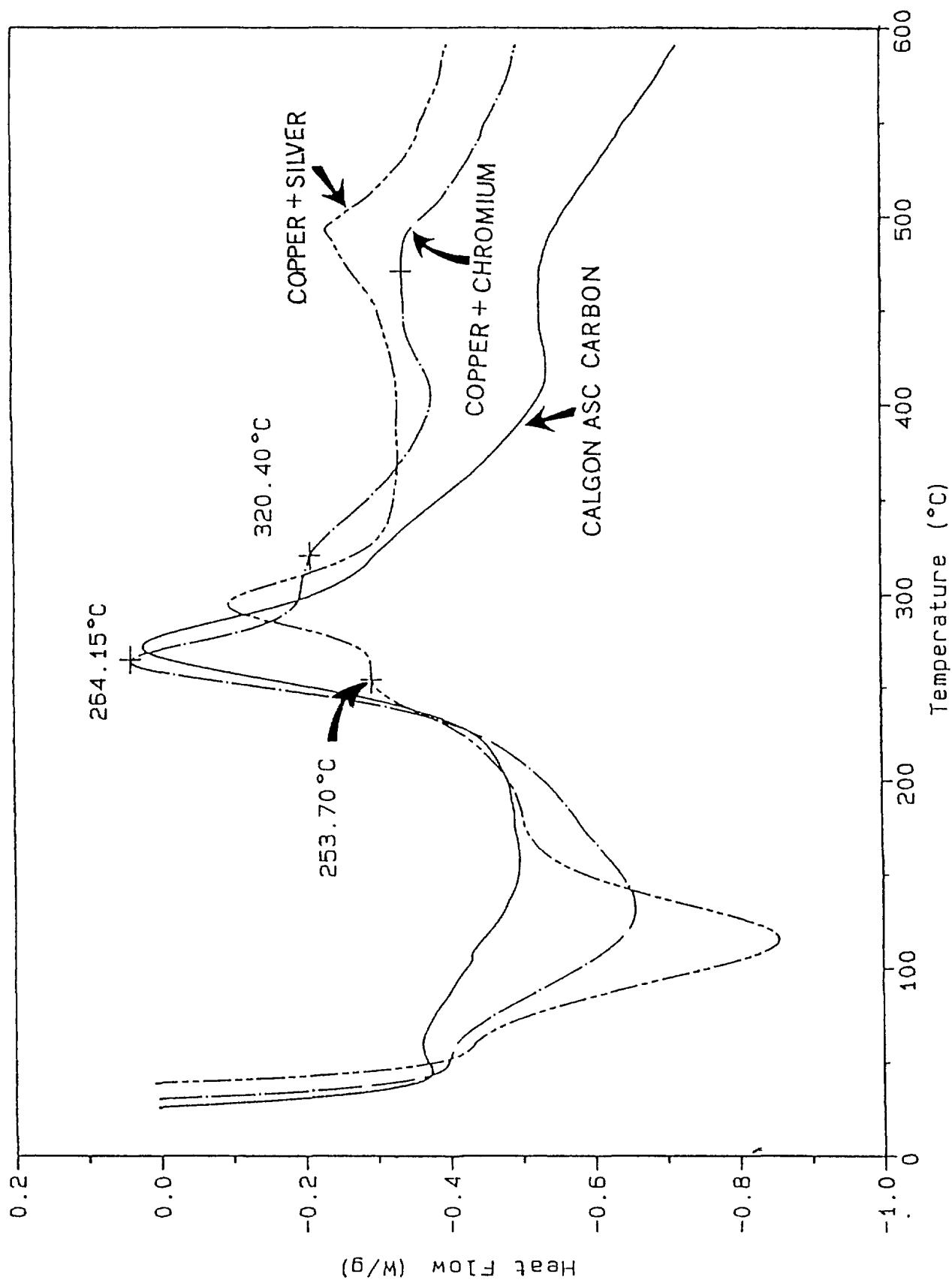


Figure 9: DSC Curves of a Copper and Chromium Impregnated Carbon vs a Calgon ASC Carbon

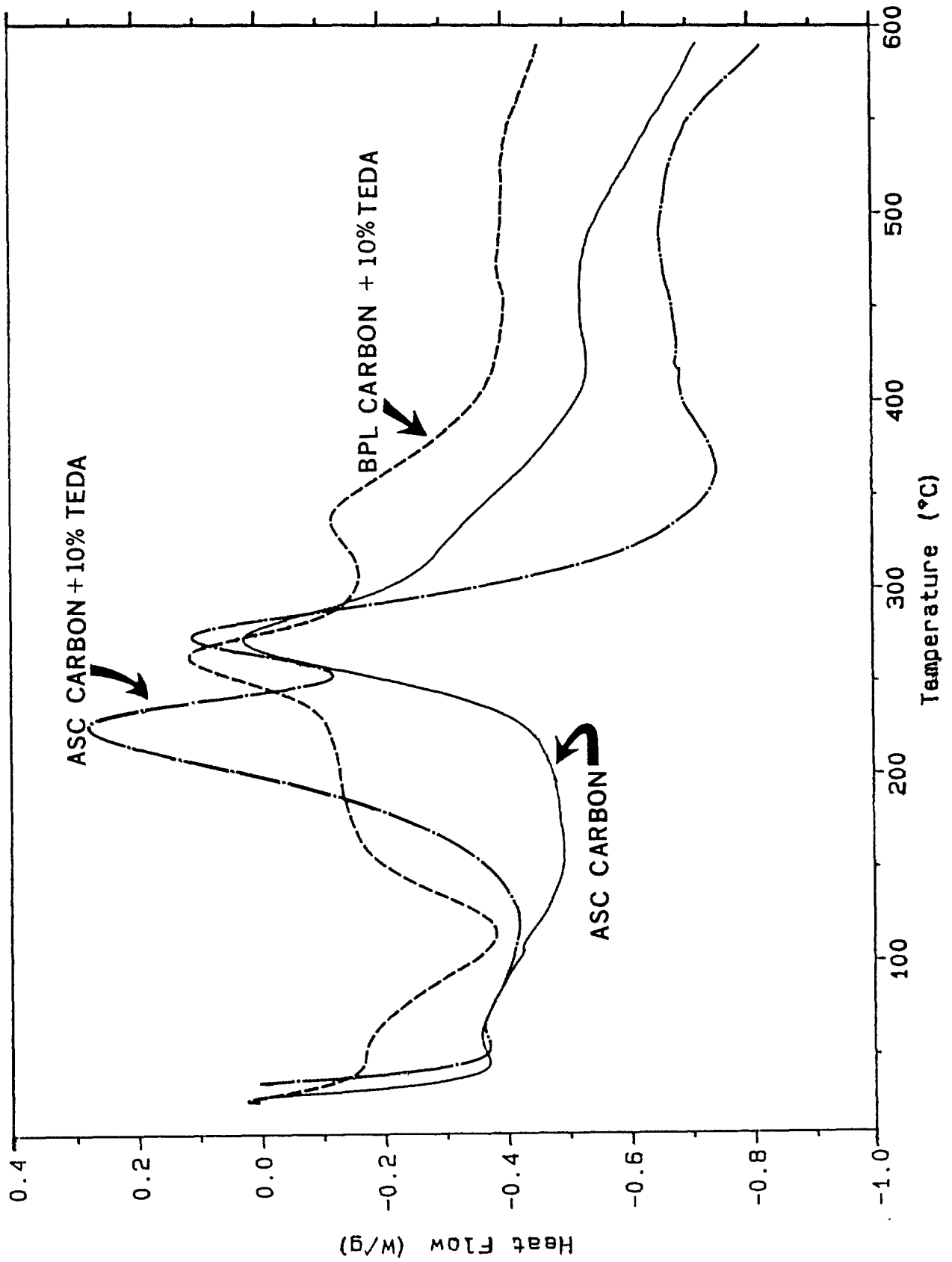


Figure 10: DSC Curves of Calgon BPL and ASC Carbons Impregnated with 10% (w/w) TEDA



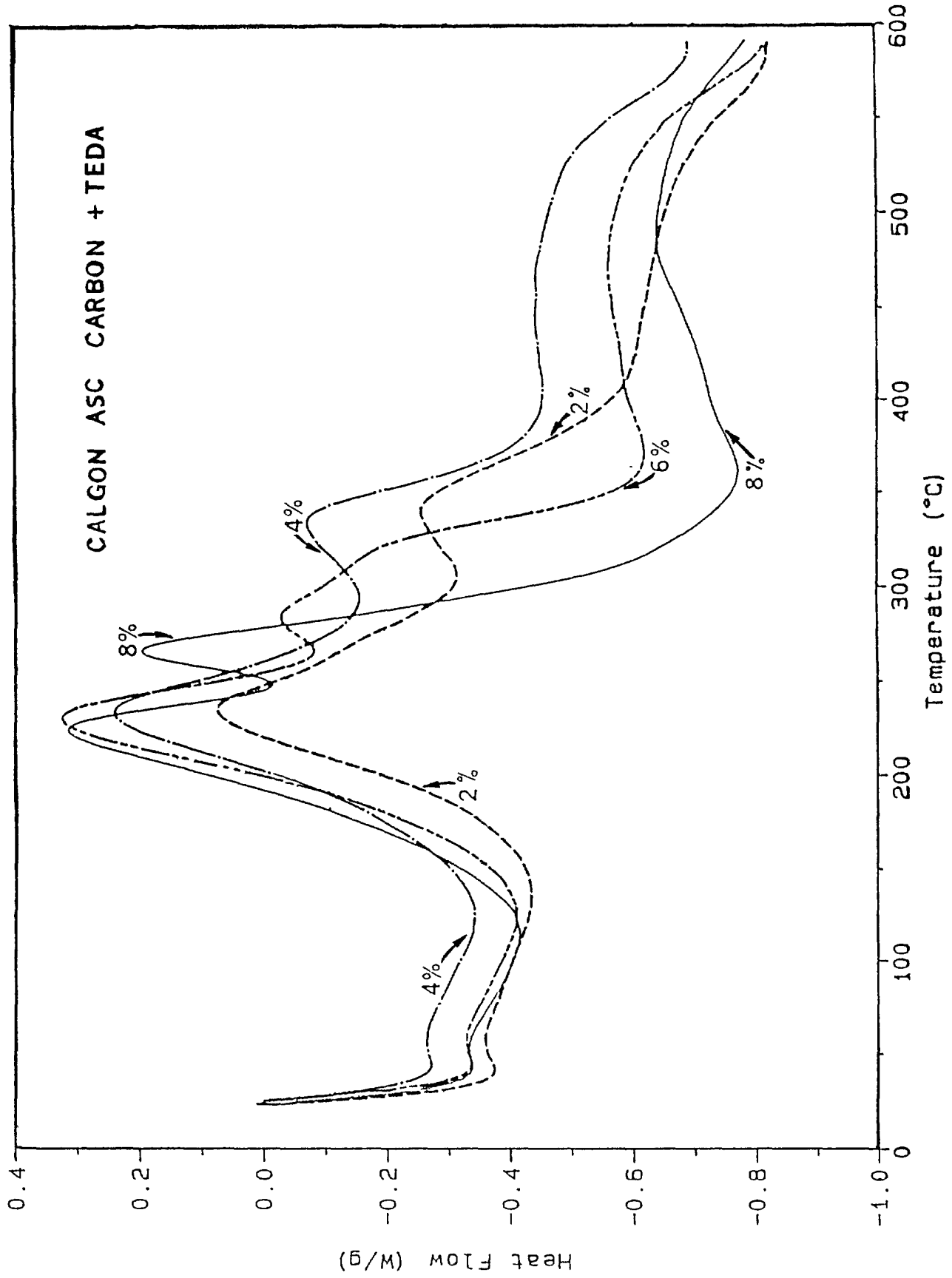


Figure 11: DSC Curves of Calgon ASC Carbons Impregnated with Various Loading Levels of TEDA

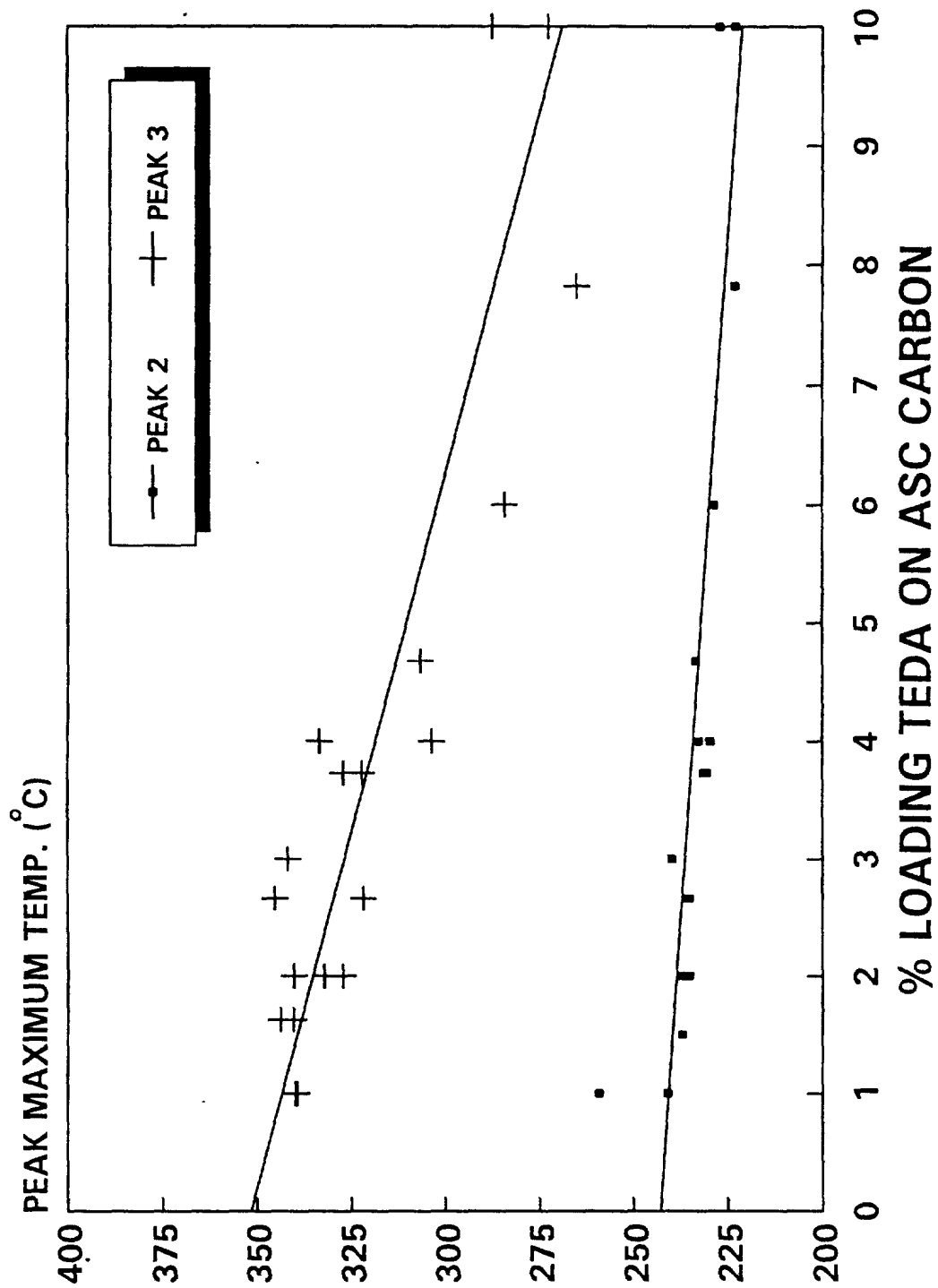


Figure 12: Peak Maximum Temperatures of the Two Exotherms on the DSC Curves versus the TEDA Loading Level

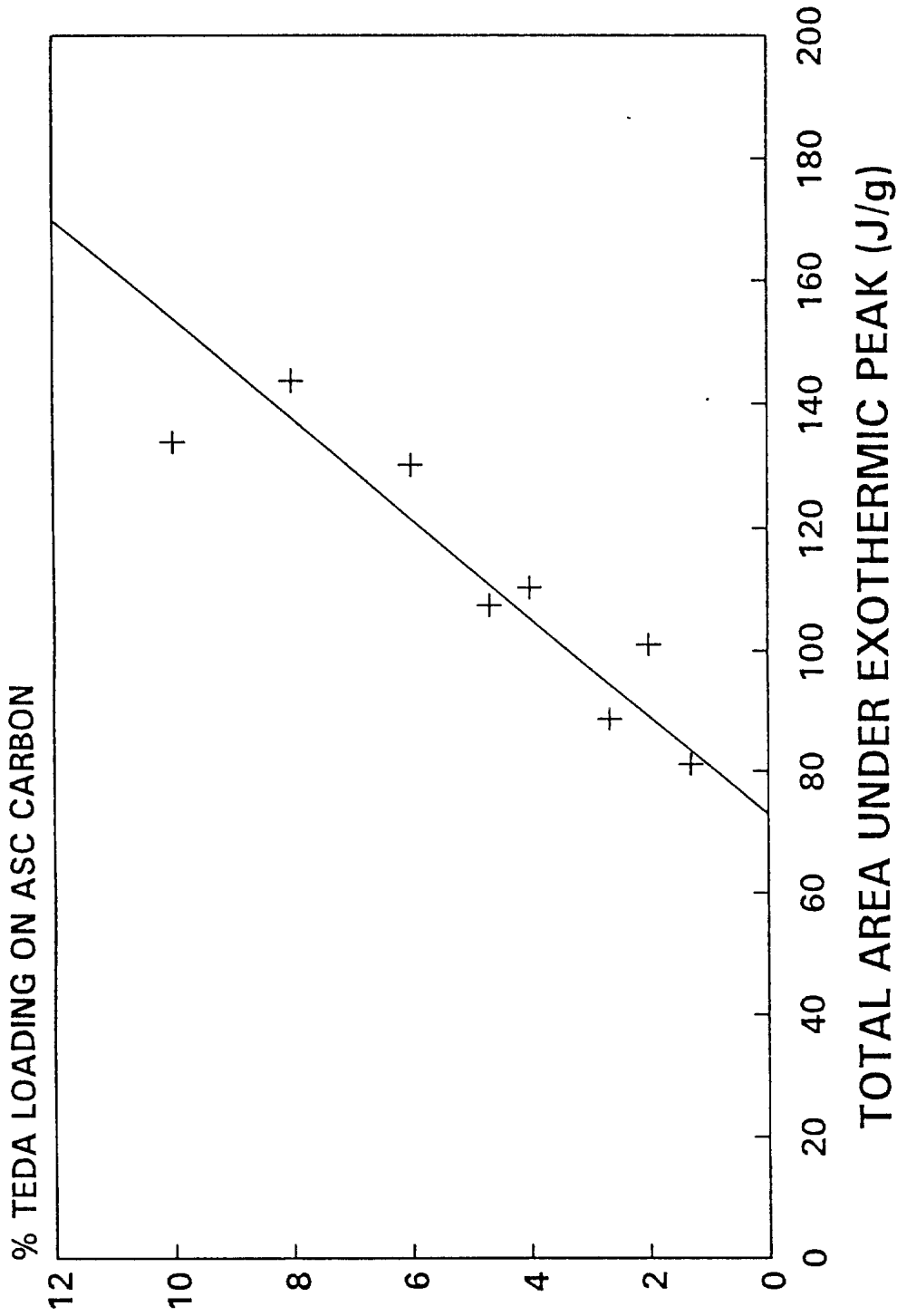


Figure 13: The Total Area of the Exotherms (peaks 2 and 3) Plotted Against Loading Level of TEDA

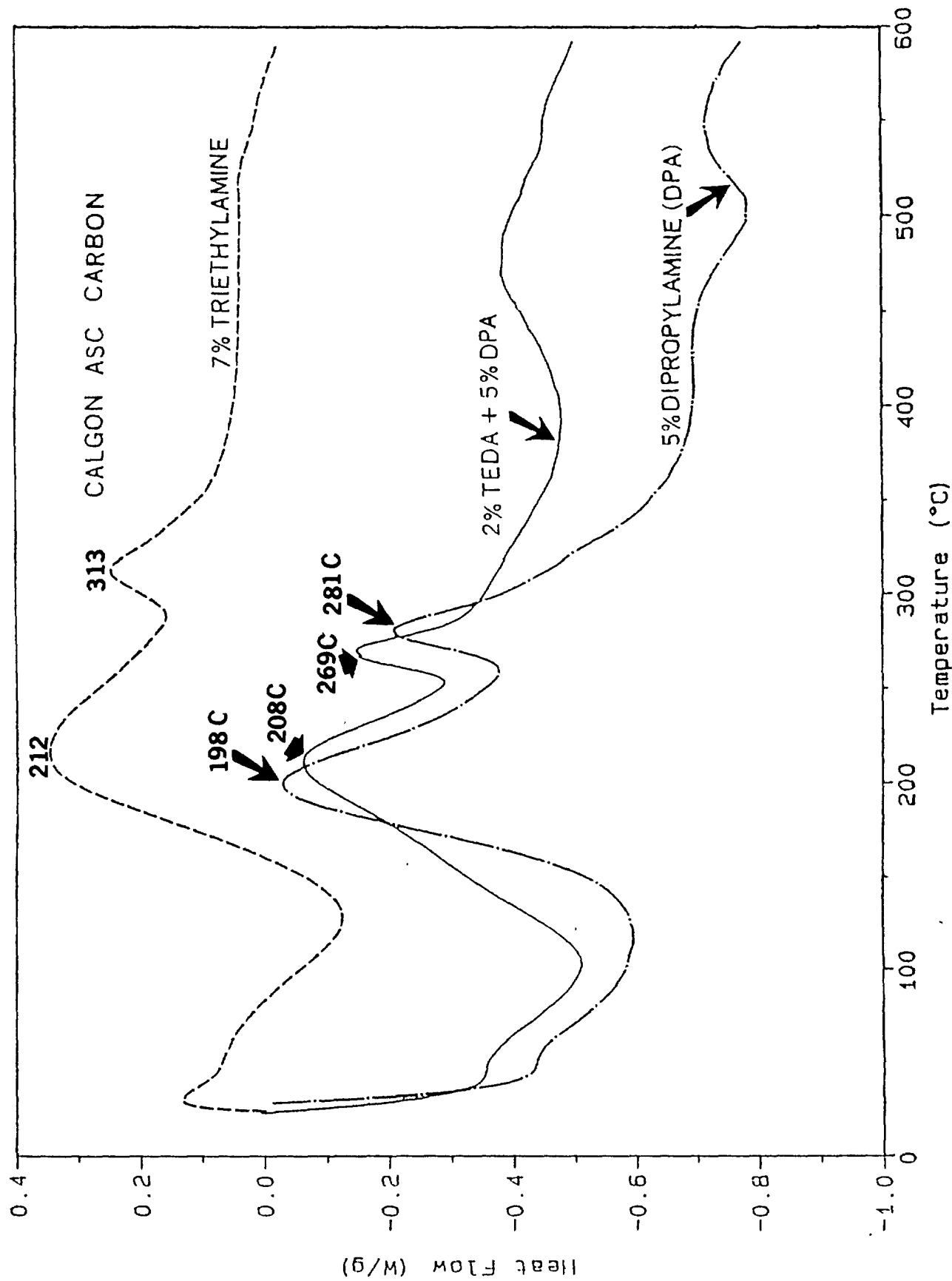


Figure 14: DSC Curves of a Calgon ASC Carbon Impregnated with Some Organic Amine Impregnants

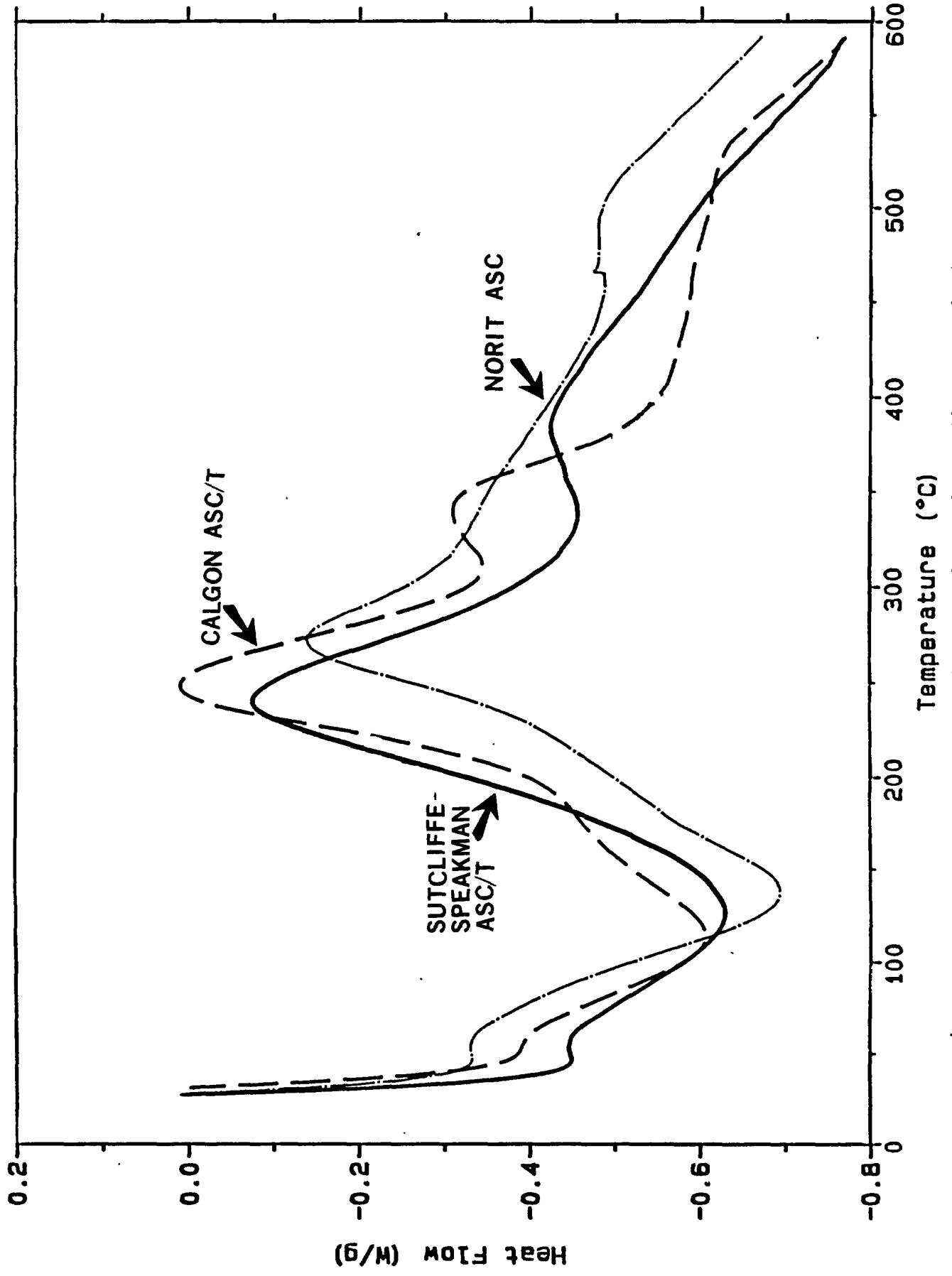


Figure 15: DSC Curves of ASC-type Carbons from Other Manufacturers

**ANNEX A****MOISTURE CONTENT DETERMINATION OF CARBON BY DSC**

For BPL and ASC carbons, it has been possible to correlate results from the ASTM method with the oven-drying methods in determining the moisture content of the carbons. However, for the ASC carbons impregnated with TEDA, such a correlation did not exist. For this reason, the feasibility of DSC for this analytical purpose was attempted. Typical DSC curves are shown in Figures A-1 to A-3 for BPL, ASC and ASC/T carbons respectively. In general, an endothermic absorption peak (i.e. a 'dip' in the DSC curve which indicates that the direction of heat flow is towards the carbon sample) occurred between 60°C and 160°C for all carbons. This was attributed to the heat required for the removal of water from the carbon surface, an explanation supported by the literature findings (10).

All carbons used in this analysis (BPL, ASC and ASC/T carbons) were pre-dried at 105°C for 3 hours. The carbon samples were stored inside glass vials fitted with ground-glass caps, and were weighed before and after the drying. Then accurately weighed water was added to the carbon, making up from 1 to 12% (by weight) of moisture on the carbon. Deionized, distilled water was used in these experiments. No trace analysis was performed on the water. It was assumed that any trace contaminant would not interfere with the DSC measurements at these water loading levels. These water-treated carbon samples were then left inside the glass vials and allowed to equilibrate inside an oven at 40°C for 3 days. DSC measurements were performed on these water-treated carbon samples from 25°C to 600°C (except ASC/T carbons which were only measured up to 250°C). The size of the first endotherm peak (corresponding to the amount of heat absorbed) increases as the amount of moisture on the carbon increases, and this was observed for all the three carbons studied (as shown in Figures A-1 to A-3).

All observed DSC curves showed an initial dip (of about 0.5 J/g), indicating that the carbon samples were being heated. The endotherm corresponding to the moisture removal from the carbon surface started at 75°C and ended at around 160°C, with the peak maximum occurring at around 100°C. The DSC curve labelled 'DRY' for all three types of carbons shown on all figures consisted of a carbon sample which was only dried at 105°C for 3 hours, thus it would still contain a fair amount of water inside the structure.

For BPL carbon, as shown in Figure A-1, all endotherms occurred at 100°C, except the carbon sample containing 5% of water for which the peak maximum occurred at ca 125°C. The same shift of the endotherm was observed on repeated runs of the same batch of carbon. This is explained as follows: at higher moisture content, (5% in this case), a higher percentage of the adsorbed water molecules would be situated inside the microstructure of the carbon. Since activated carbon itself is a poor conductor of heat, it would take more time for the heat to transfer from the carbon surface to the inner structure so that the water molecules can be evaporated and removed. Furthermore, the carbon sample was heated at a rate of 30°C/minute (therefore the temperature axis is also, in a sense, a time axis), a longer heating period would then imply a higher temperature at which the endotherm occurred. BPL carbon samples with added water as high as 20% by weight, showed an endotherm at ca 150°C, confirming this explanation. This shift of the endotherm attributed to water removal, is not as pronounced as in the case for ASC and ASC/T carbons. In general, this endotherm occurred at ca 125°C for ASC and 150 °C for ASC/T carbons. This higher temperature (or longer heating period) at which the water is removed from the carbon surface is the result of the stronger interaction between the water molecules and the metal impregnants on the carbon surface, rather than the amount of water present. This explanation is supported by the fact that: 1) the endotherm did not shift to higher temperature at higher loading level of water; and 2) because of the ionic nature of the metal impregnants, the sites on the carbon surface which are occupied by the metal offer stronger interaction to the water molecules because of their polar nature.

The moisture content of the carbon was then plotted against the heat absorbed in this endothermic change (i.e. the area underneath the endotherms on the DSC curve). The plots are shown in Figure A-4 for all three carbons, which in general show a linear relationship. None of the regression lines passed through the origin, because the carbon which was labelled 'dry' was only dried at 105°C for 3 hours, and could still contain a substantial amount of water in the pore structures. Regression analysis using a first-order least squares fit was applied to all three relationships, and the following results were obtained:

BPL	:	$Y = -0.520 + 0.0702X$	$(R^2=0.997)$	[A-1]
ASC	:	$Y = -2.003 + 0.0729X$	$(R^2=0.990)$	[A-2]
ASC/T	:	$Y = -0.800 + 0.0914X$	$(R^2=0.978)$	[A-3]

Note that the linear regression used all the data up to 5% moisture only. The data corresponding to higher moisture content (e.g. 12% for ASC carbon) was put on the regressed line afterwards, and was not used in the regression model. This observation, combined with the very good regression coefficient ( $R^2$ ) show that a reasonable linearity exists. Furthermore, this indicates that moisture content can be extrapolated from the regression model, if the heat absorbed (i.e. the area of the endotherm under the DSC curve) due to water removal is obtained by DSC measurement. The standard deviation associated with the determination of the area under the DSC curve has been estimated to be  $\pm 15\%$  (as detailed in Section 4 of this report). Thus, the moisture content on the carbon surface determined by DSC analysis would have an uncertainty of about  $\pm 15\%$ . This precision was not improved by using a slower rate of heating as was also confirmed by the French researchers (10).

Notice that the slope has the following units:

$$(\text{g of water}) \times 100\% / (\text{g of carbon}) \div (\text{joule}) / (\text{g of carbon}) \quad [\text{A-4}]$$

Therefore, the reciprocal of the slope of the regression model will have units of joule/(100 g of water), and may be interpreted as the heat required to release the surface water ( $H_{\text{water}}$ ). For the three carbons employed in this study, this amount of heat is equal to 79.09, 76.24 and 60.77 Joule/mole for BPL, ASC and ASC/T carbons respectively. The reason for assigning this as the heat associated with the release of surface water is that the value of 79 J/mole obtained for BPL carbon is about two orders of magnitude lower than the heat of adsorption of water ( $H_{\text{ads}}$ ) reported by Barton (23).

If the water added to all the carbon samples can be assumed to be a liquid water layer on the carbon surface (without any physical or chemical interaction with the surface), then the minimum heat required to remove it can be calculated as follows:

$$H_{\text{vap}} = (\text{g of water}) (\text{specific heat of water}) (\text{temp. change}) \\ + (\text{g water}) (\text{latent heat of vaporization}) \quad [\text{A-5}]$$

A sample calculation involving a carbon sample (normally about 16.5 mg in each DSC run from 25 to 100°C) with a 1% moisture content, and assuming that carbon did not pick up any appreciable amount of heat, is shown as follows:

$$H_{\text{vap}} = 0.01 \times 0.0165 \times 1.00 \times (100-25) \\ + 0.01 \times 0.0165 \times 540 \text{ cal} \\ = 0.1015 \text{ cal} \\ = 0.424 \text{ J}$$



This calculation shows that the numbers calculated for  $H_{\text{water}}$  above probably corresponds to the heat of physical adsorption of water, i.e. water which is: i) not chemically adsorbed on the carbon surface; ii) not in the microporous structure of the carbon (which is difficult to remove); and iii) not labile enough to behave like liquid water.

Another interesting feature of Figure A-4 is that it appears that water is more strongly 'physically-bound' to ASC carbon than on either BPL or ASC/T carbon. This is based on the difference of the slopes of the lines, and the intercept (on the x-axis). At 0% moisture (as was pointed out earlier, the carbon was not really 'dry' at 0% moisture), ASC carbon has a x-intercept of 25 J/g, while about 8 J/g for both BPL and ASC/T carbons. This probably indicates different levels of interaction between water and the carbon surfaces on these three carbons.

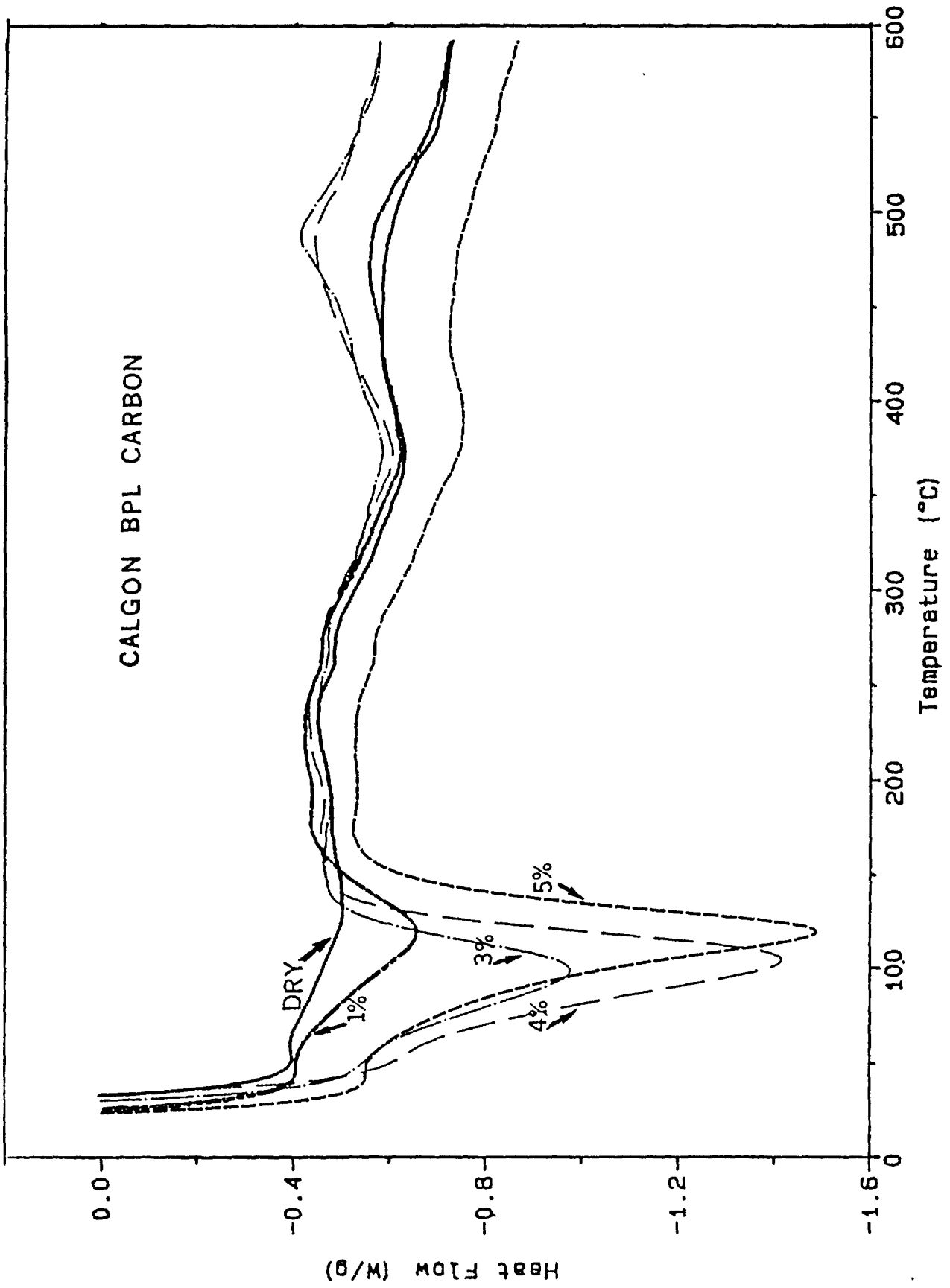


Figure A-1: Variation of DSC Curves with the Amount of Added Water for Calgon BPL Carbon

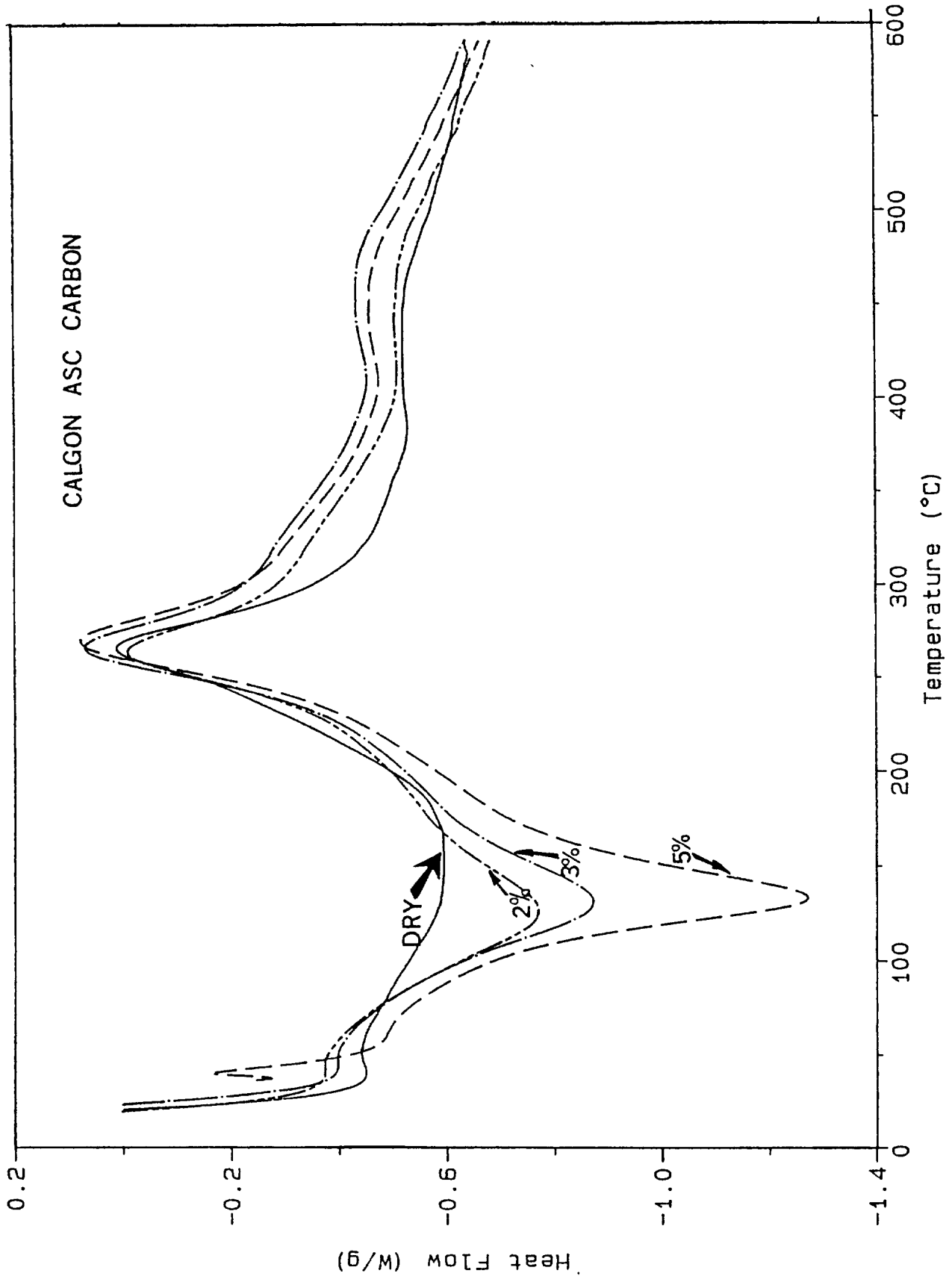


Figure A-2: Variation of DSC Curves with the Amount of Added Water for Calgon ASC Carbon

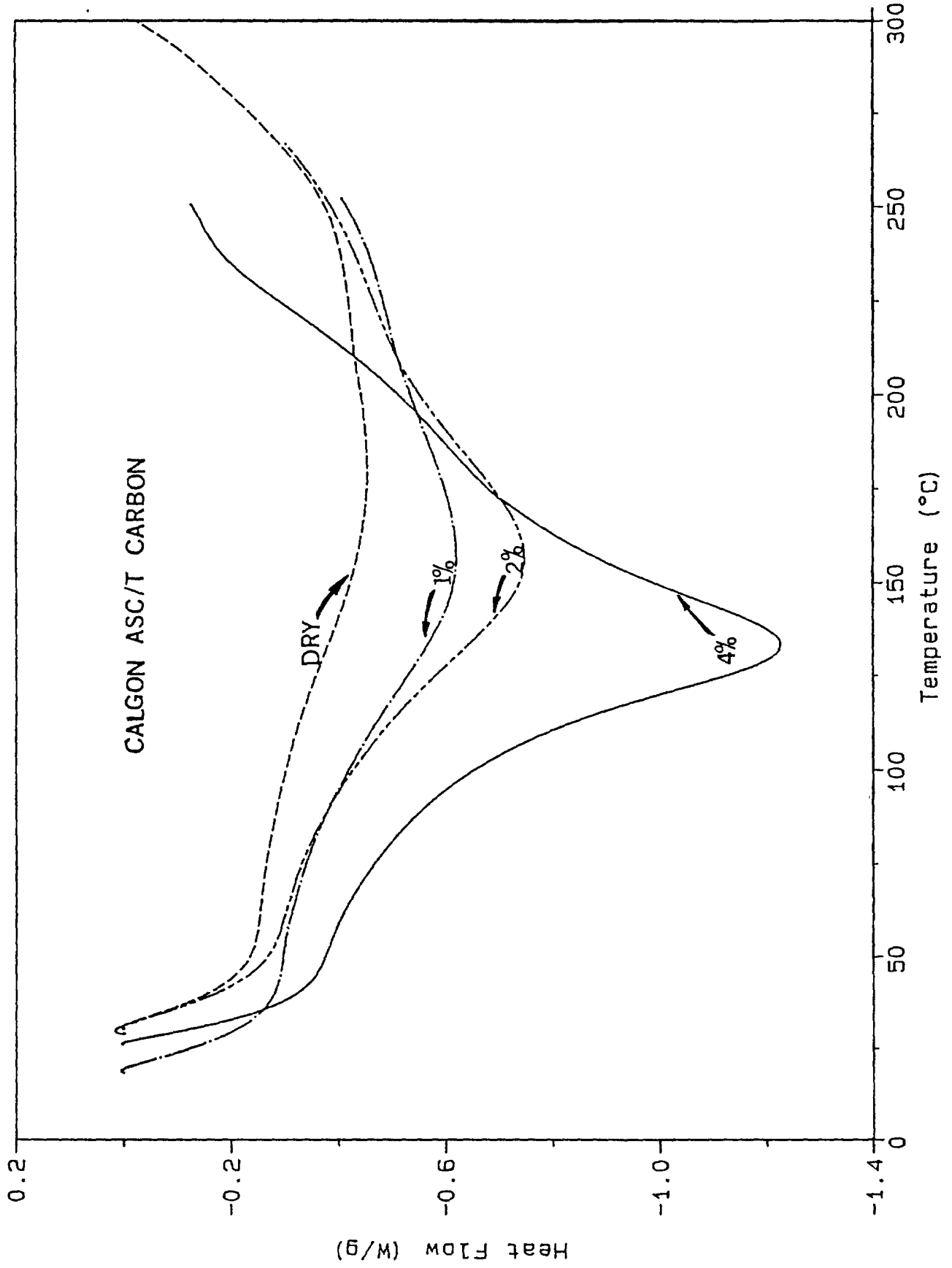


Figure A-3: Variation of DSC Curves with the Amount of Added Water for Calgon ASC/T Carbon

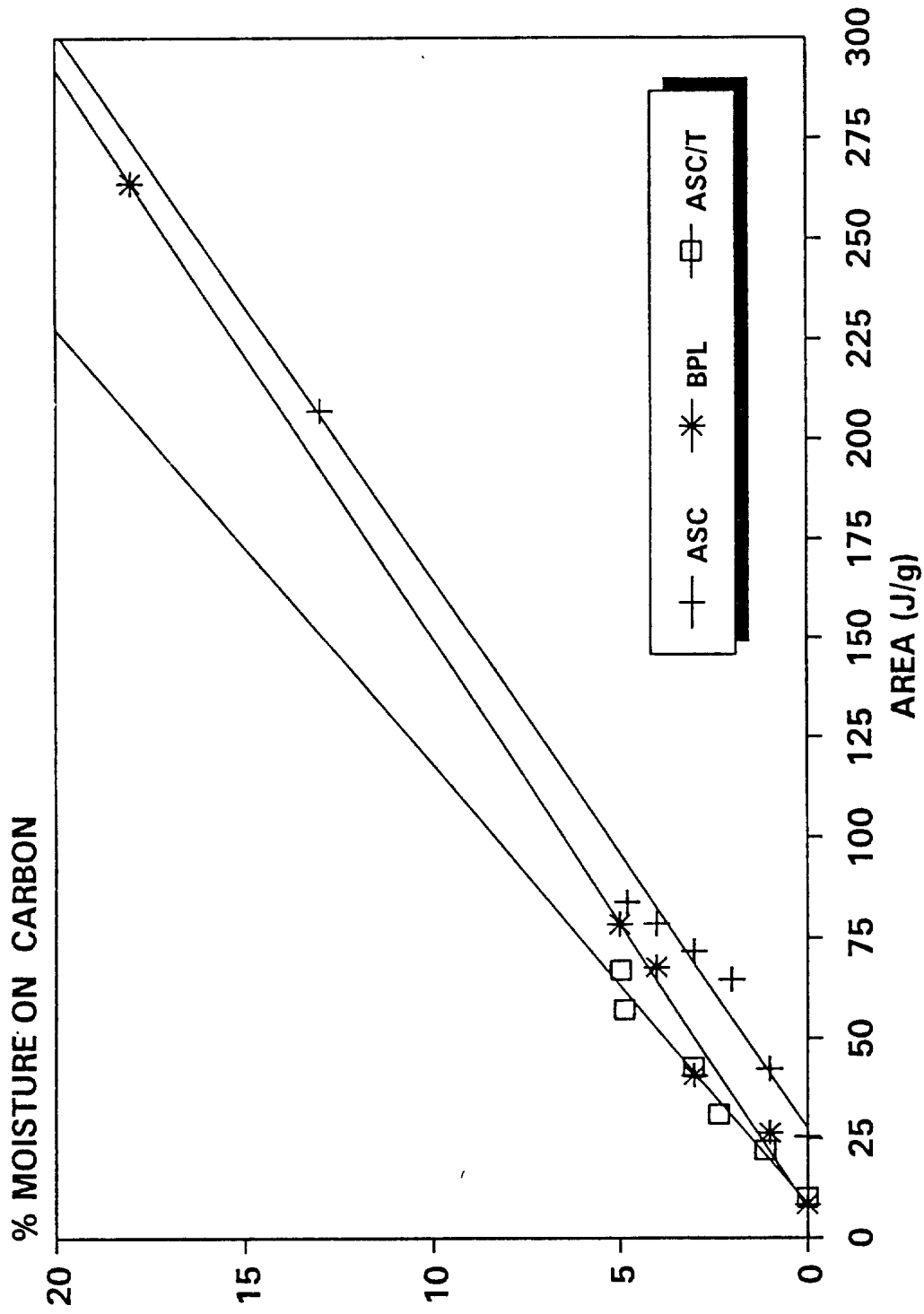


Figure A-4: Plots of Percentage Moisture Content Versus the Area Under the DSC Curve for Calgon BPL, ASC and ASC/T Carbons

UNCLASSIFIED

-47-

SECURITY CLASSIFICATION OF FORM  
(highest classification of Title, Abstract, Keywords)

## DOCUMENT CONTROL DATA

(Security classification of title, body of abstract and indexing annotation must be entered when the overall document is classified)

1. ORIGINATOR (the name and address of the organization preparing the document. Organizations for whom the document was prepared, e.g. Establishment sponsoring a contractor's report, or tasking agency, are entered in section 8.) DEFENCE RESEARCH ESTABLISHMENT OTTAWA National Defence Ottawa, Ontario K1A 0Z4		2. SECURITY CLASSIFICATION (overall security classification of the document, including special warning terms if applicable)  UNCLASSIFIED	
3. TITLE (the complete document title as indicated on the title page. Its classification should be indicated by the appropriate abbreviation (S,C or U) in parentheses after the title.)  DIFFERENTIAL SCANNING CALORIMETRY (DSC) FOR THE ANALYSIS OF ACTIVATED CARBON (U)			
4. AUTHORS (Last name, first name, middle initial)  LIANG, Septimus H.C. and CAMERON, Laura E.			
5. DATE OF PUBLICATION (month and year of publication of document)  OCTOBER	6a. NO. OF PAGES (total containing information. Include Annexes, Appendices, etc.)  53	6b. NO. OF REFS (total cited in document)  23	
7. DESCRIPTIVE NOTES (the category of the document, e.g. technical report, technical note or memorandum. If appropriate, enter the type of report, e.g. interim, progress, summary, annual or final. Give the inclusive dates when a specific reporting period is covered.)  REPORT			
8. SPONSORING ACTIVITY (the name of the department project office or laboratory sponsoring the research and development. Include the address.)  DEFENCE RESEARCH ESTABLISHMENT OTTAWA National Defence Ottawa, Ontario K1A 0Z4			
9a. PROJECT OR GRANT NO. (if appropriate, the applicable research and development project or grant number under which the document was written. Please specify whether project or grant)  051LD		9b. CONTRACT NO. (if appropriate, the applicable number under which the document was written)	
10a. ORIGINATOR'S DOCUMENT NUMBER (the official document number by which the document is identified by the originating activity. This number must be unique to this document.)  DREO REPORT NO. 1098		10b. OTHER DOCUMENT NOS. (Any other numbers which may be assigned this document either by the originator or by the sponsor)	
11. DOCUMENT AVAILABILITY (any limitations on further dissemination of the document, other than those imposed by security classification)  <input checked="" type="checkbox"/> Unlimited distribution <input type="checkbox"/> Distribution limited to defence departments and defence contractors; further distribution only as approved <input type="checkbox"/> Distribution limited to defence departments and Canadian defence contractors; further distribution only as approved <input type="checkbox"/> Distribution limited to government departments and agencies; further distribution only as approved <input type="checkbox"/> Distribution limited to defence departments; further distribution only as approved <input type="checkbox"/> Other (please specify):			
12. DOCUMENT ANNOUNCEMENT (any limitation to the bibliographic announcement of this document. This will normally correspond to the Document Availability (11). However, where further distribution (beyond the audience specified in 11) is possible, a wider announcement audience may be selected.)			

UNCLASSIFIED

SECURITY CLASSIFICATION OF FORM

DCD03 2/06/87

UNCLASSIFIED

SECURITY CLASSIFICATION OF FORM

13. ABSTRACT ( a brief and factual summary of the document. It may also appear elsewhere in the body of the document itself. It is highly desirable that the abstract of classified documents be unclassified. Each paragraph of the abstract shall begin with an indication of the security classification of the information in the paragraph (unless the document itself is unclassified) represented as (S), (C), or (U). It is not necessary to include here abstracts in both official languages unless the text is bilingual).

SO // The technique of Differential Scanning Calorimetry (DSC) has been applied to the characterization and the analysis of several activated carbons. These activated carbons included BPL carbon (a base carbon), ASC carbon (a BPL carbon impregnated with copper, chromium and silver) and ASC/T carbon (an ASC carbon impregnated with triethylenediamine, TEDA). DSC has been shown to be capable of measuring enthalpic changes associated with transitions and/or reactions of the surface species on the activated carbon. Physical changes or chemical reactions occurring on the carbon surface and the surface impregnants are observed as endotherms or exotherms (enthalpic changes) on the DSC curves (thermograms). The data from this study have demonstrated that DSC can be used quantitatively in the determination of the amount of TEDA impregnant on the activated carbon surface. This is based on the linear relationship between the area under the DSC curve and the amount of TEDA present. Qualitatively, DSC is shown to be able to differentiate between carbons which have been impregnated with different organic and/or metal impregnants, because each impregnated carbon produces a DSC thermogram which is unique to the compounds on its surface. This is due to the fact that different impregnants react with the carbon surface at different temperatures, thus giving rise to different DSC curves. It has also been found that activated carbons produced from different manufacturers showed different enthalpic characteristics.

14. KEYWORDS, DESCRIPTORS or IDENTIFIERS (technically meaningful terms or short phrases that characterize a document and could be helpful in cataloguing the document. They should be selected so that no security classification is required. Identifiers, such as equipment model designation, trade name, military project code name, geographic location may also be included. If possible keywords should be selected from a published thesaurus. e.g. Thesaurus of Engineering and Scientific Terms (TEST) and that thesaurus-identified. If it is not possible to select indexing terms which are Unclassified, the classification of each should be indicated as with the title.)

ACTIVATED CARBON  
DIFFERENTIAL SCANNING CALORIMETRY  
IMPREGNANTS (INORGANIC/ORGANIC)  
TRIETHYLENEDIAMINE

92-00681  
# 103575

UNCLASSIFIED

SECURITY CLASSIFICATION OF FORM